

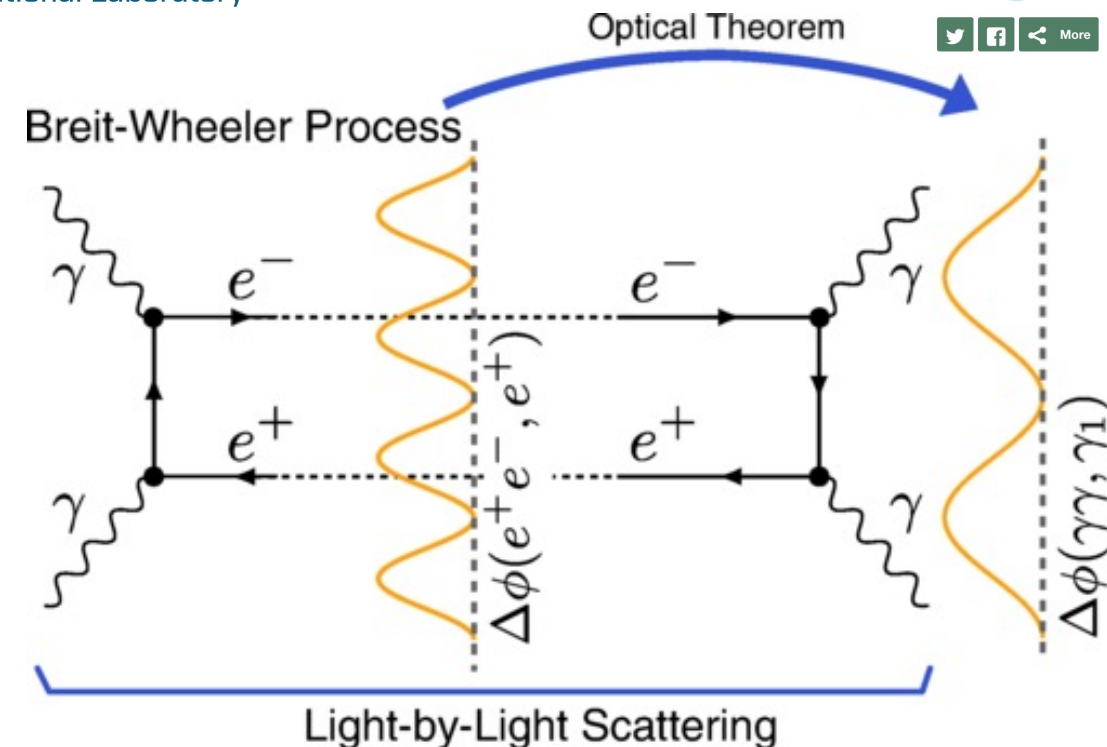
# Map EM field in Heavy-ion collisions with Breit-Wheeler Process

- Basic pure EM process in Heavy-ion collisions
- Constrain charge radius at RHIC
  - UPC
  - Centrality
  - beam energy dependence
- Final-state EM field
- Charge vs baryon stopping, opportunity with isobar data

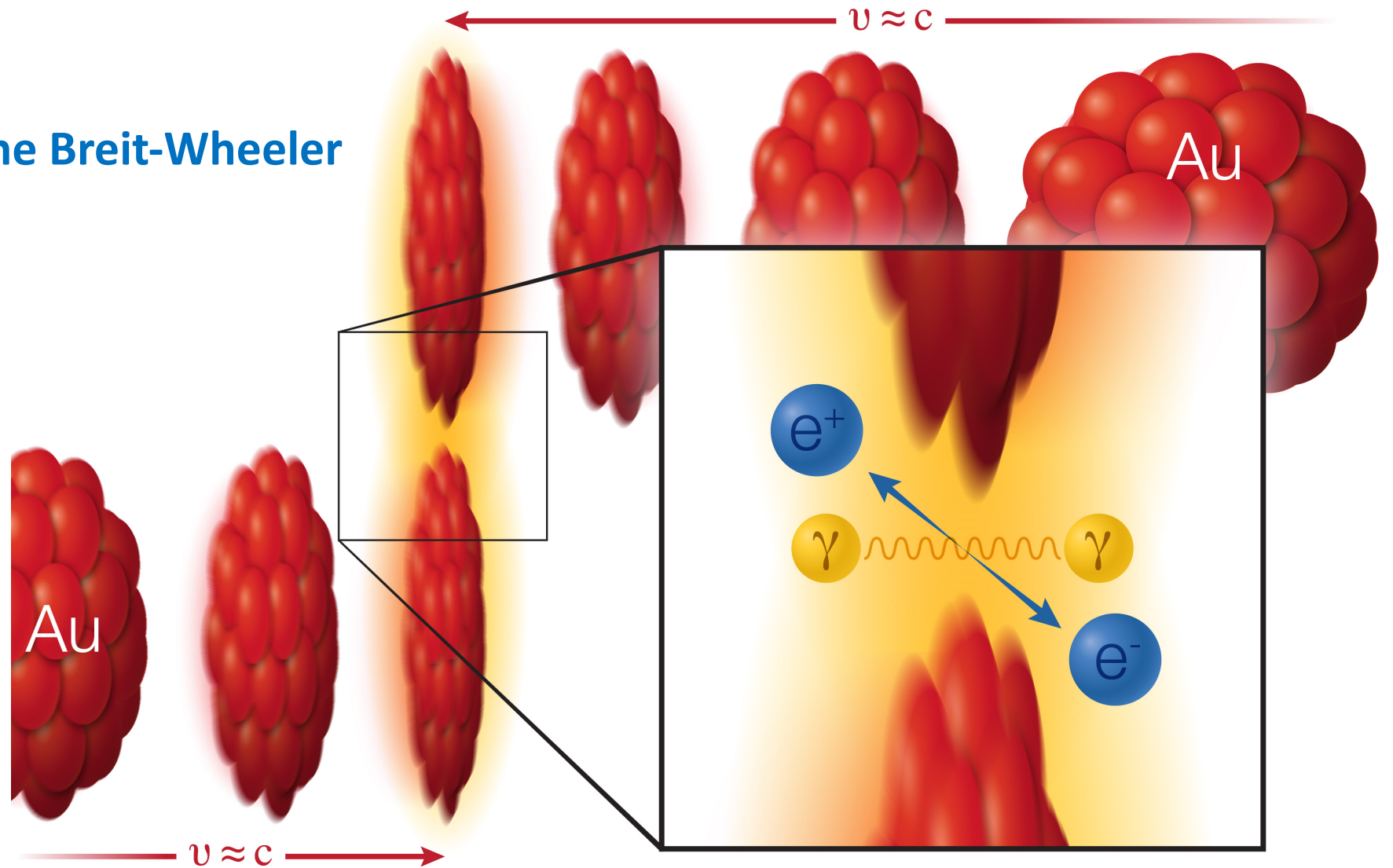
Zhangbu Xu



[arXiv:1806.02295](#) PRL  
[arXiv:1804.01813](#) PLB  
[arXiv:1705.01460](#) PRC  
[arXiv:1812.02820](#) PLB  
[arXiv:1910.12400](#) PRL  
[arXiv:2103.16623](#) EPJA  
STAR BUR 2017-2021

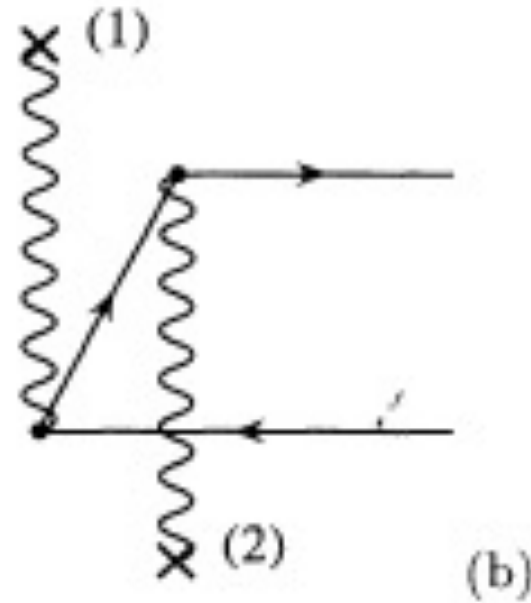
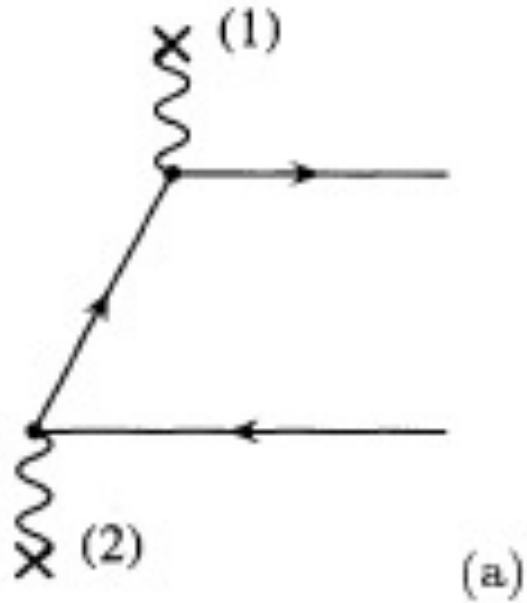


## First, some basics of the Breit-Wheeler process



Two gold (Au) ions (red) move in opposite direction at 99.995% of the speed of light ( $v$ , for velocity, = approximately  $c$ , the speed of light). As the ions pass one another without colliding, two photons ( $\gamma$ ) from the electromagnetic cloud surrounding the ions can interact with each other to create a matter-antimatter pair: an electron ( $e^-$ ) and positron ( $e^+$ ).

# Lowest-order QED calculation



$$\sigma = \int d^2b \frac{d^6 P(\vec{b})}{d^3p_+ d^3p_-} = \int d^2q \frac{d^6 P(\vec{q})}{d^3p_+ d^3p_-} \int d^2b e^{i\vec{q} \cdot \vec{b}}$$

$$\begin{aligned} \frac{d^6 P(\vec{q})}{d^3p_+ d^3p_-} &= (Z\alpha)^4 \frac{4}{\beta^2} \frac{1}{(2\pi)^6 2\epsilon_+ 2\epsilon_-} \int d^2q_1 \\ &F(N_0)F(N_1)F(N_3)F(N_4)[N_0N_1N_3N_4]^{-1} \\ &\times \text{Tr}\{(\not{p}_- + m)[N_{2D}^{-1}\not{p}_1(\not{p}_- - \not{q}_1 + m)\not{p}_2 + \\ &N_{2X}^{-1}\not{p}_2(\not{q}_1 - \not{p}_+ + m)\not{p}_1](\not{p}_+ - m)[N_{5D}^{-1}\not{p}_2 \\ &(\not{p}_- - \not{q}_1 - \not{q} + m)\not{p}_1 + N_{5X}^{-1}\not{p}_1(\not{q}_1 + \not{q} - \not{p}_+ \\ &+ m)\not{p}_2]\}, \end{aligned}$$

with

$$\begin{aligned} N_0 &= -q_1^2, N_1 = -[q_1 - (p_+ + p_-)]^2, \\ N_3 &= -(q_1 + q)^2, N_4 = -[q + (q_1 - p_+ - p_-)]^2, \\ N_{2D} &= -(q_1 - p_-)^2 + m^2, \\ N_{2X} &= -(q_1 - p_+)^2 + m^2, \\ N_{5D} &= -(q_1 + q - p_-)^2 + m^2, \\ N_{5X} &= -(q_1 + q - p_+)^2 + m^2, \end{aligned}$$

# Initial Transverse Momentum Broadening

$$\begin{aligned} \sigma = & 16 \frac{Z^4 e^4}{(4\pi)^2} \int d^2 b \int \frac{dw_1}{w_1} \frac{dw_2}{w_2} \frac{d^2 k_{1\perp}}{(2\pi)^2} \frac{d^2 k_{2\perp}}{(2\pi)^2} \frac{d^2 q_{\perp}}{(2\pi)^2} \\ & \times \frac{F(-k_1^2)}{k_1^2} \frac{F(-k_2^2)}{k_2^2} \frac{F^*(-k_1'^2)}{k_1'^2} \frac{F^*(-k_2'^2)}{k_2'^2} e^{-i\vec{b} \cdot \vec{q}_{\perp}} \\ & \times [(\vec{k}_{1\perp} \cdot \vec{k}_{2\perp})(\vec{k}'_{1\perp} \cdot \vec{k}'_{2\perp})\sigma_s(w_1, w_2) \\ & + (\vec{k}_{1\perp} \times \vec{k}_{2\perp})(\vec{k}'_{1\perp} \times \vec{k}'_{2\perp})\sigma_{ps}(w_1, w_2)] \end{aligned} \quad (2)$$

Zha, et al., arXiv: 1812.02820

M. Vidovic, et al., Phys.Rev. C47 (1993) 2308

$$\rho_A(r) = \frac{\rho^0}{1 + \exp[(r - R_{WS})/d]}$$

$$dn_i = \frac{Z_i^2 \alpha}{\pi^2} \frac{q_{i\perp}^2 \left[ F\left(q_{i\perp}^2 + \frac{w_i^2}{\gamma^2}\right) \right]^2}{\left(q_{i\perp}^2 + \frac{w_i^2}{\gamma^2}\right)^2} \frac{d^3 q_i}{w_i} \quad (1)$$

arXiv:1005.3531, unpublished

$$\begin{aligned} \sigma = & 16 \frac{Z^4 e^4}{(4\pi)^2} \int \frac{dw_1}{w_1} \frac{dw_2}{w_2} \frac{d^2 k_{1\perp}}{(2\pi)^2} \frac{d^2 k_{2\perp}}{(2\pi)^2} \left| \frac{F(-k_1^2)}{k_1^2} \right|^2 \\ & \times \left| \frac{F(-k_2^2)}{k_2^2} \right|^2 k_{1\perp}^2 k_{2\perp}^2 \sigma(w_1, w_2) \end{aligned} \quad (6)$$

S. Klein, et al. Comput.Phys.Commun. 212 (2017) 258-268

**Is photon pt really driven by uncertainty principle  
and independent of position-momentum correlation?**

we can afford many mistakes in the search.  
The main thing is to make them as fast as possible.

– John Archibald Wheeler

[doi:10.1063/1.3120895](https://doi.org/10.1063/1.3120895)

$\omega/\gamma \lesssim k t \ll \omega$

Higher-order/virtuality cancels to  $1/\gamma^2 \sim 10^{-4}$

NLO QED coupling constant  $\alpha=1/137$



# Electron Identification

TPC dE/dx: large hadron background

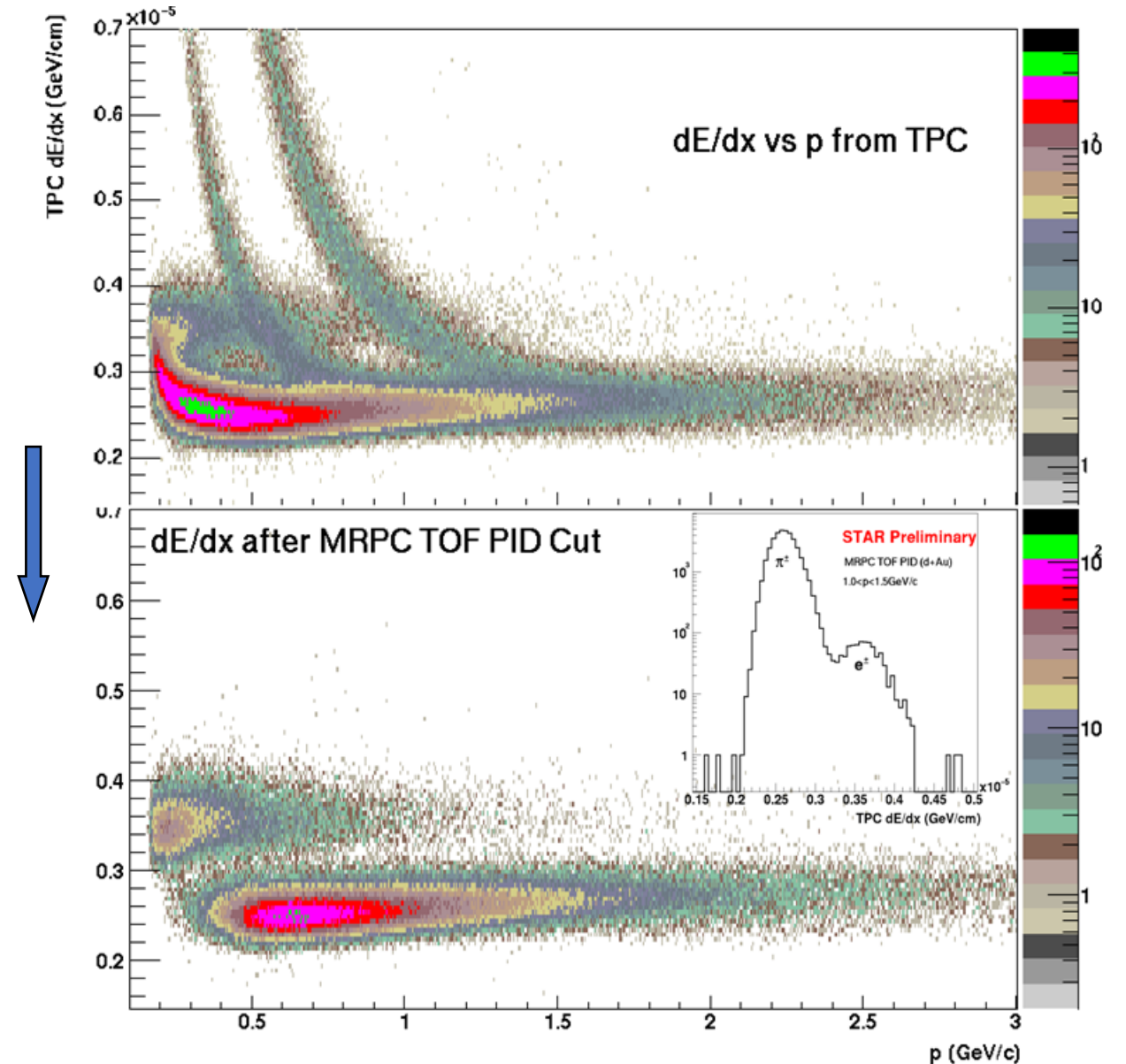
EMC:  $p_T > \sim 2.0$  GeV/c

A prototype TOF tray (TOFr) in 2003  
TOF is not always the obvious choice  
but it has proven to be crucial for STAR

$$|1/\beta - 1| < 0.03$$

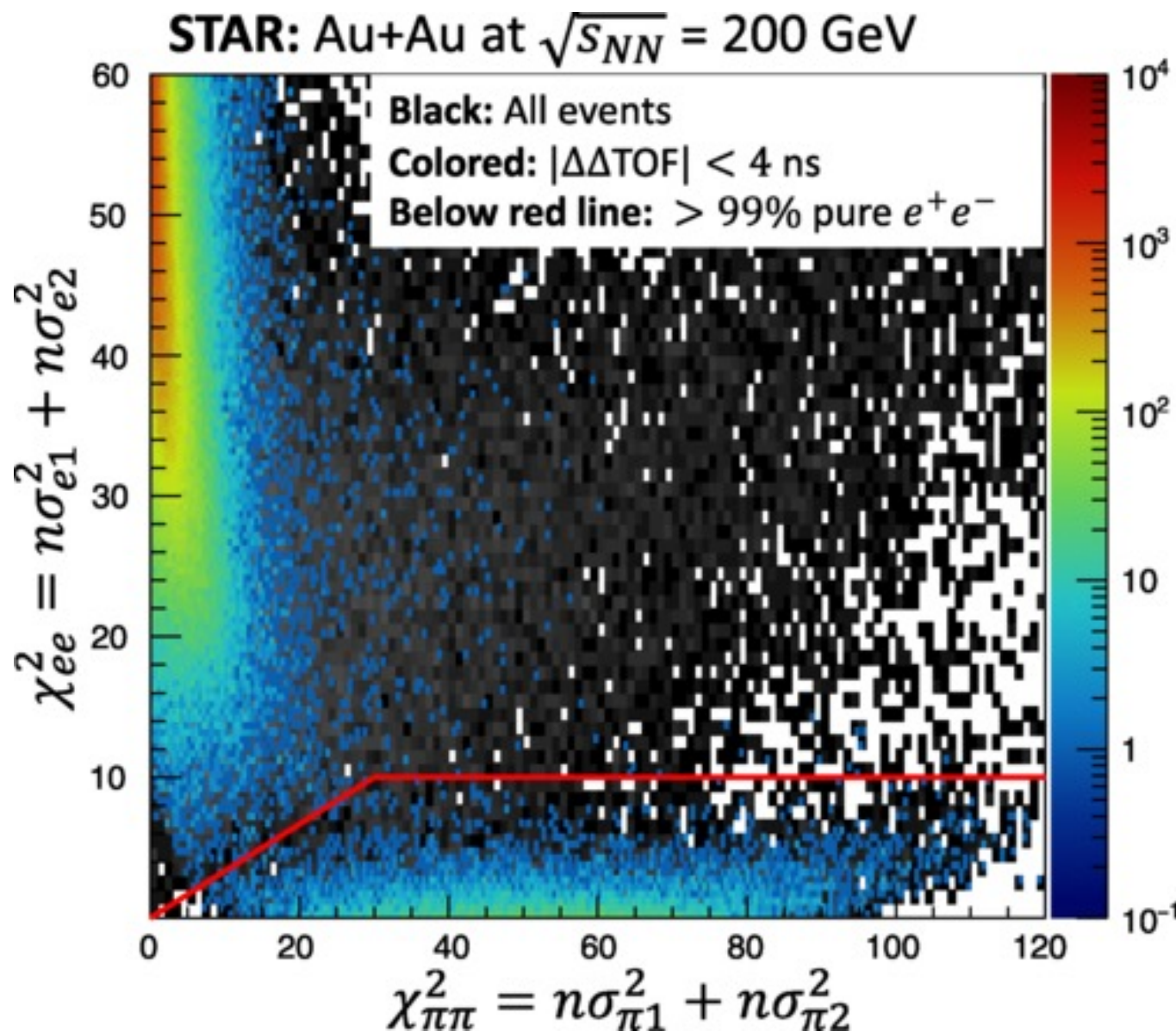
Not able to do without TOF!

nucl-ex/0505026, M. Shao et al.  
X. Dong PHD Thesis (USTC 2005)  
L. Ruan PHD Thesis (USTC 2004)



# Reject Hadronic Background

J. Adam *et al.* (STAR Collaboration)  
Phys. Rev. Lett. **127** (2021) 052302



From  $\pi/e > 100$

To  $\pi/e < 1/100$

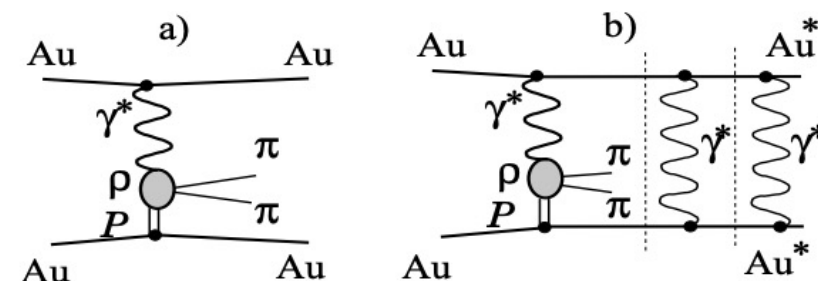


FIG. 1: Diagram for (a) exclusive  $\rho^0$  production in ultra-peripheral heavy ion collisions, and (b)  $\rho^0$  production with nuclear excitation. The dashed lines indicate factorization.

Phys. Rev. Lett. **89** (2002) 272302

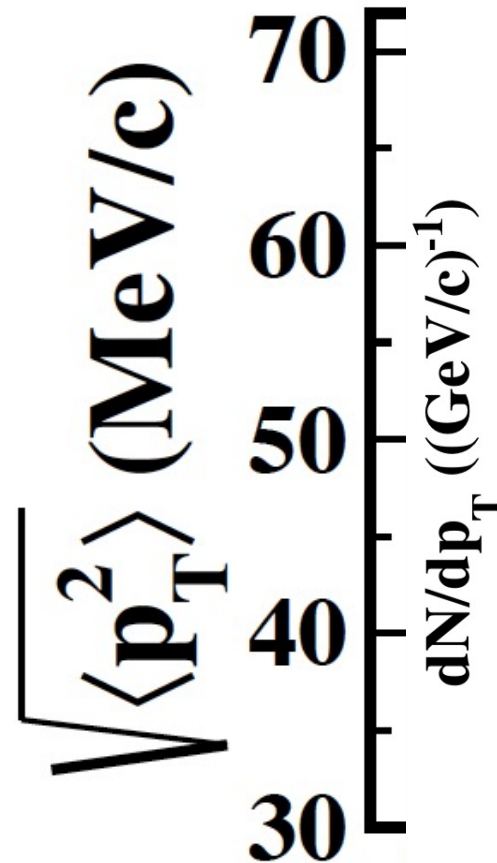
# $p_T$ broadening

Two Issues:

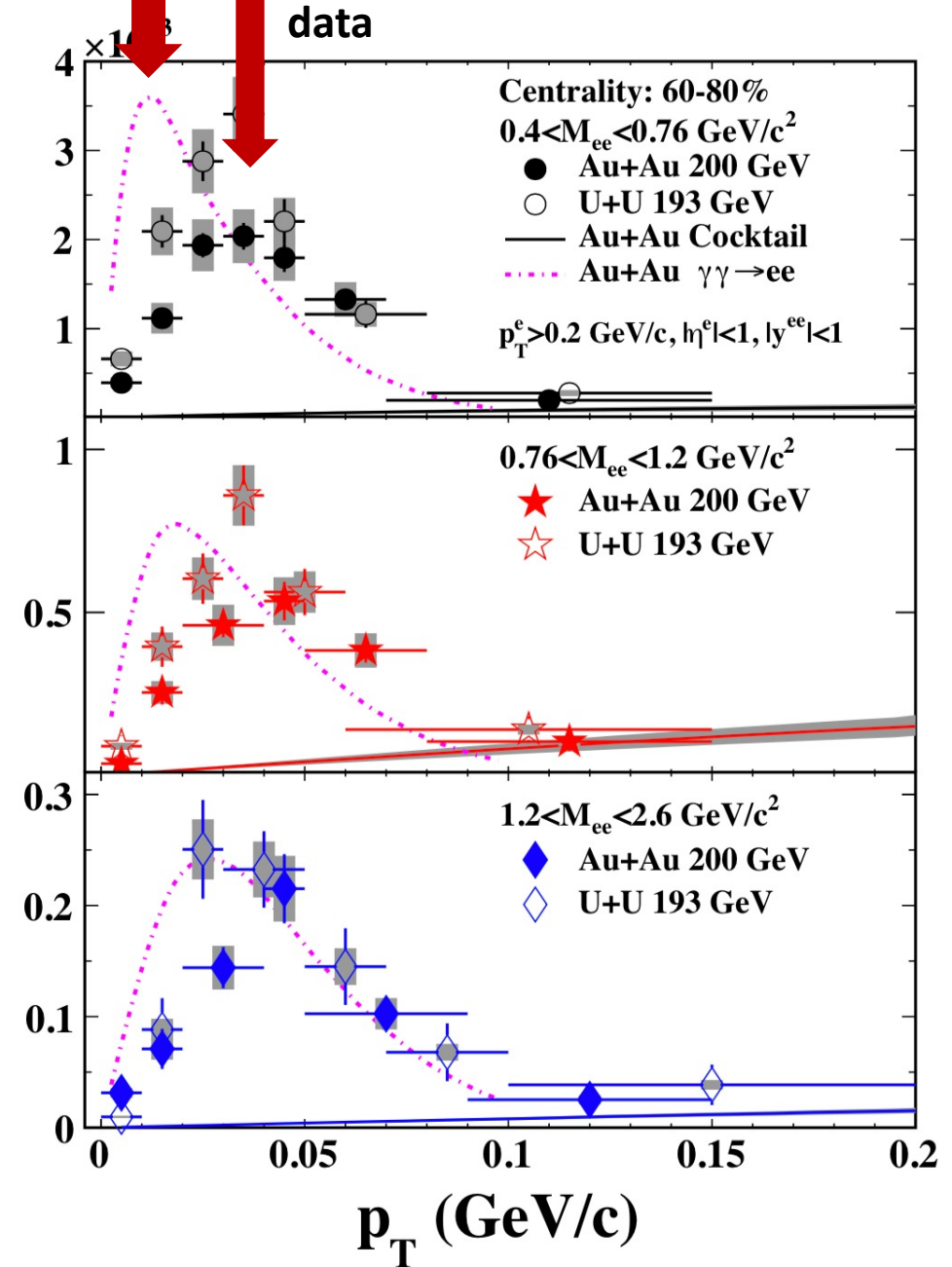
$p_T$  spread ( $\sigma_t$ ) > Model  
additional broadening of 40 MeV

Au+Au > U+U

Why “broadening”:  
Gaussian in  $p_T$



STARlight Model



5



# What did STAR say in the publication?


PHYSICAL REVIEW LETTERS **121**, 132301 (2018)

---

## Low- $p_T$ $e^+e^-$ Pair Production in Au + Au Collisions at $\sqrt{s_{NN}} = 200$ GeV and U + U Collisions at $\sqrt{s_{NN}} = 193$ GeV at STAR

PHYSICAL REVIEW LETTERS **121**, 132301 (2018)

---

 (Received 6 June 2018; revised manuscript received 30 August 2018; published 25 September 2018)

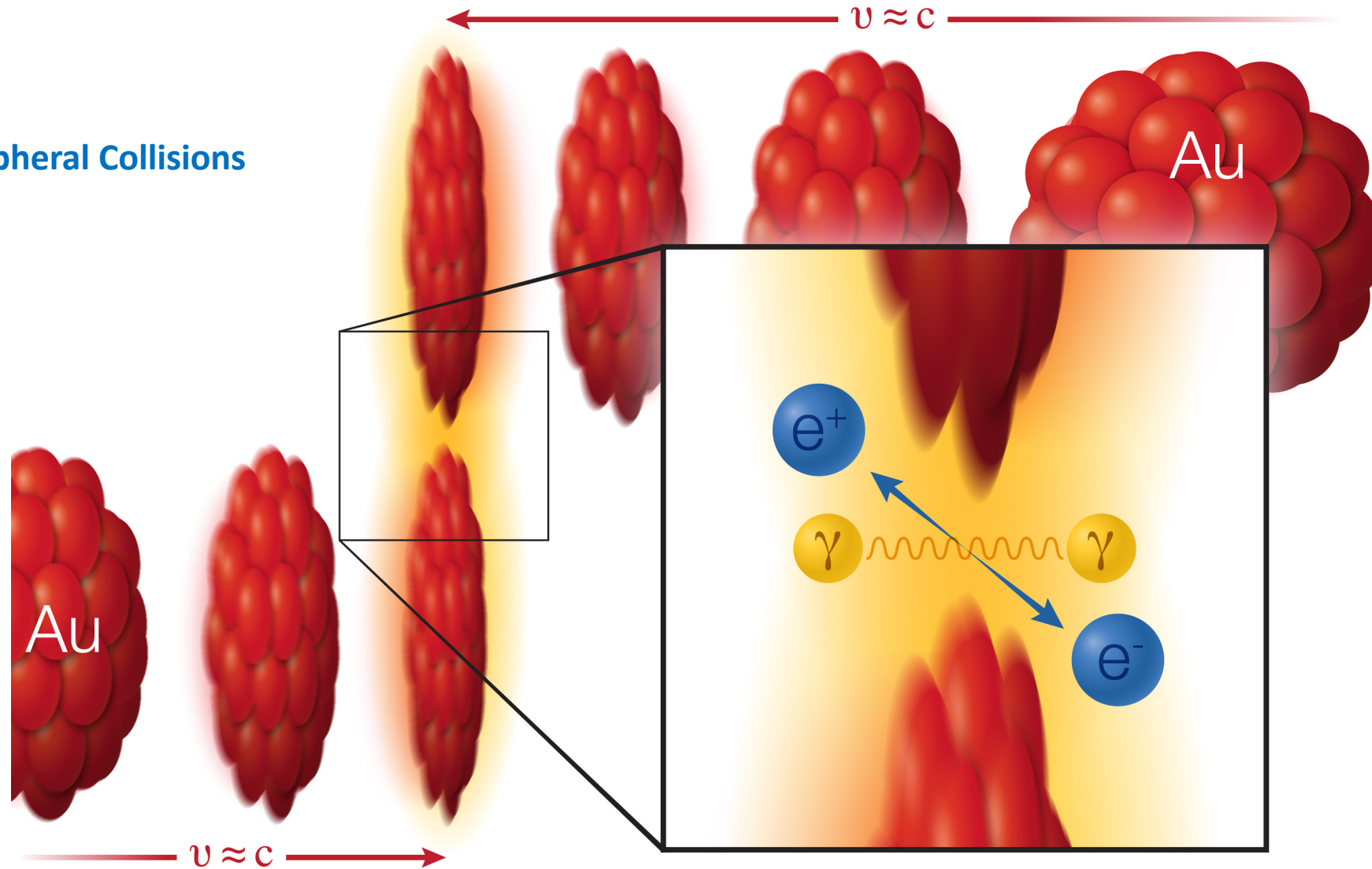
We report first measurements of  $e^+e^-$  pair production in the mass region  $0.4 < M_{ee} < 2.6$  GeV/ $c^2$  at low transverse momentum ( $p_T < 0.15$  GeV/ $c$ ) in noncentral Au + Au collisions at  $\sqrt{s_{NN}} = 200$  GeV and U + U collisions at  $\sqrt{s_{NN}} = 193$  GeV. Significant enhancement factors, expressed as ratios of data over known hadronic contributions, are observed in the 40%–80% centrality of these collisions. The excess yields peak distinctly at low  $p_T$  with a width ( $\sqrt{\langle p_T^2 \rangle}$ ) between 40 and 60 MeV/ $c$ . The absolute cross section of the excess depends weakly on centrality, while those from a theoretical model calculation incorporating an in-medium broadened  $\rho$  spectral function and radiation from a quark gluon plasma or hadronic cocktail contributions increase dramatically with an increasing number of participant nucleons. Model calculations of photon-photon interactions generated by the initial projectile and target nuclei describe the observed excess yields but fail to reproduce the  $p_T^2$  distributions.

DOI: 10.1103/PhysRevLett.121.132301

Fig. 4(d). For example, to illustrate the sensitivity the  $\sqrt{\langle p_T^2 \rangle}$  measurement may have to a postulated magnetic field trapped in a conducting QGP [21], we assume each and every pair member generated by model [33] traverses 1 fm through a constant magnetic field of  $10^{14}$  T perpendicular to the beam line ( $eBL \approx 30$  MeV/ $c$ , where  $B$  is  $10^{14}$  T,  $L$  is 1 fm) [37, 38]. The corresponding  $p_T^2$  distributions of  $e^+e^-$  pairs can qualitatively describe our data except at low  $p_T^2$ , as shown in Figs. 4(a)-(c). The  $\sqrt{\langle p_T^2 \rangle}$  of  $e^+e^-$  pairs will gain an additional  $\sim 30$  MeV/ $c$ , as illustrated in Fig. 4(d). This level of broadening is measurable and may indicate the possible existence of high magnetic fields [21, 37, 38].

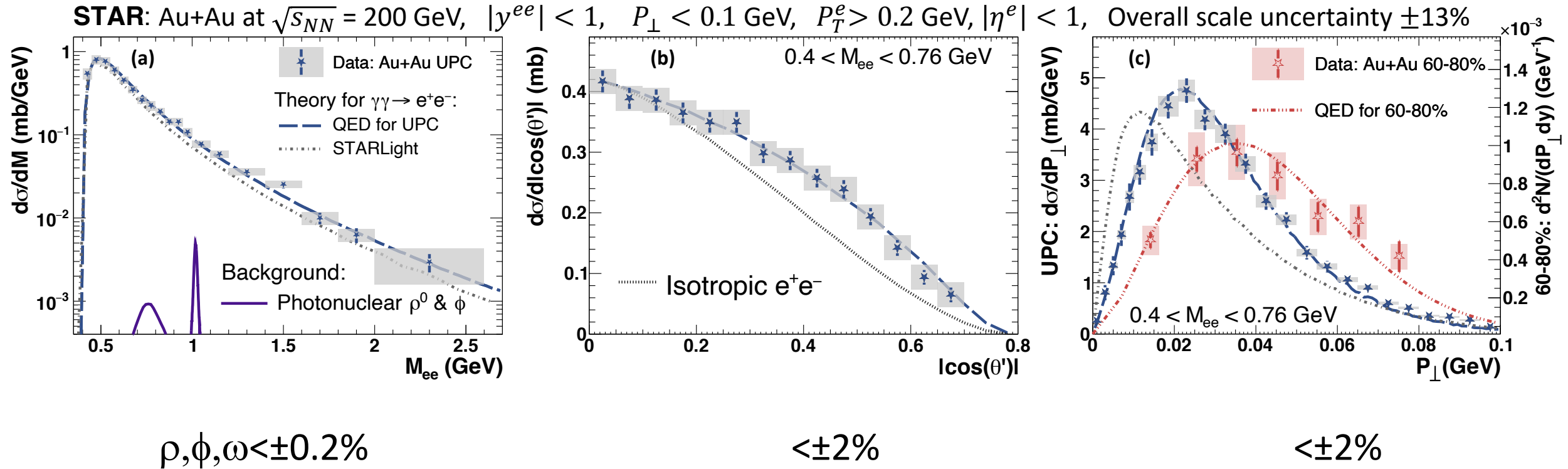


## Ultra-Peripheral Collisions



Two gold (Au) ions (red) move in opposite direction at 99.995% of the speed of light ( $v$ , for velocity, = approximately  $c$ , the speed of light). As the ions pass one another without colliding, two photons ( $\gamma$ ) from the electromagnetic cloud surrounding the ions can interact with each other to create a matter-antimatter pair: an electron ( $e^-$ ) and positron ( $e^+$ ).

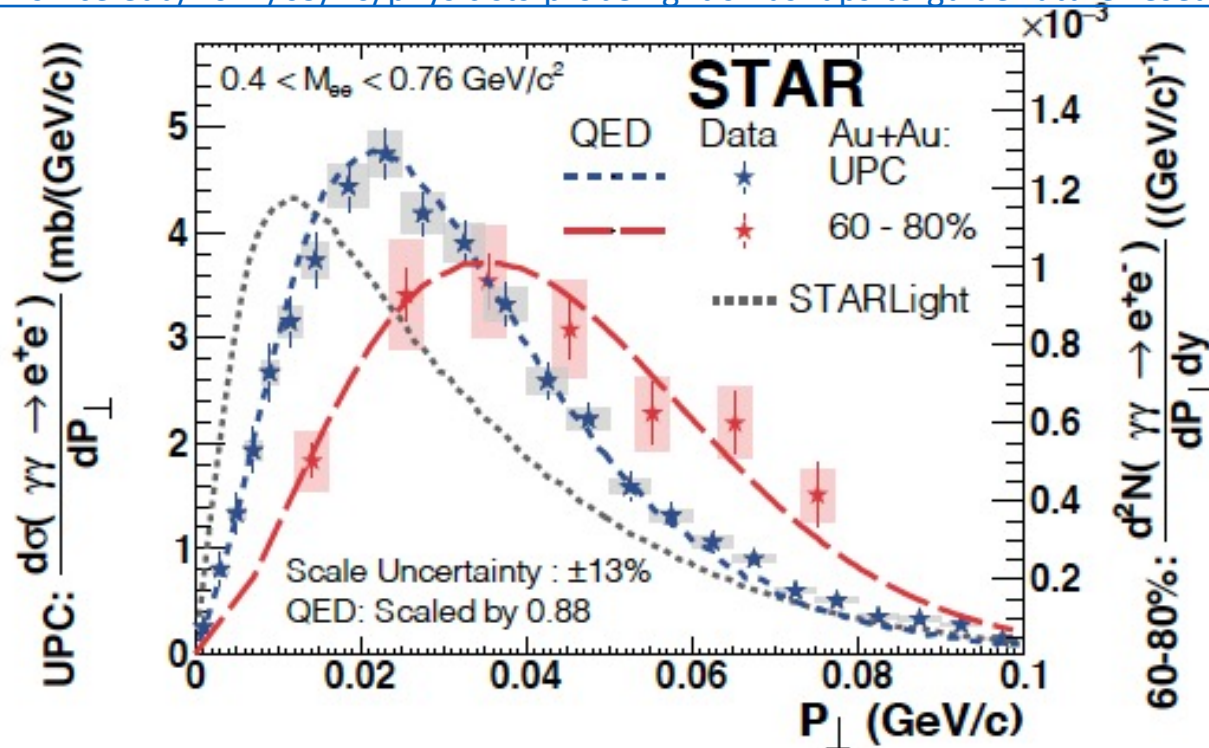
# Well understood kinematics



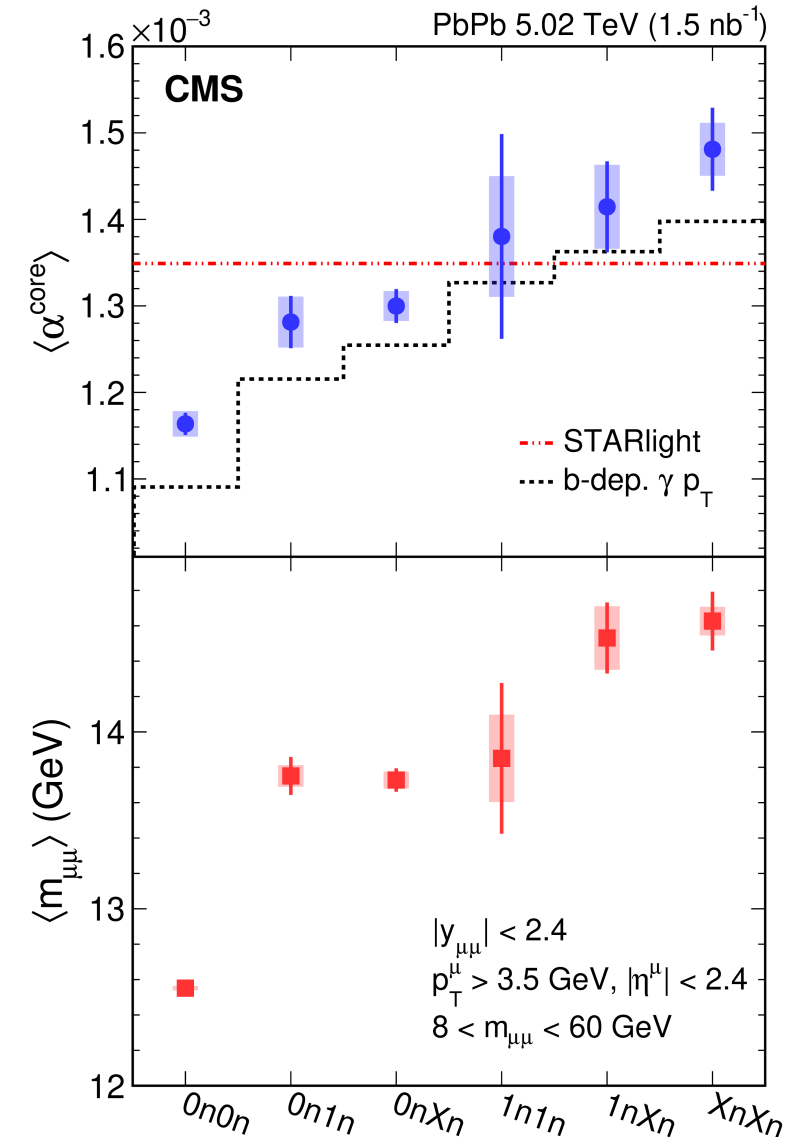
# Photon TMD in UPC

CMS Abstract: “This observation demonstrates the transverse momentum and energy of photons emitted from relativistic ions have impact parameter dependence. These results constrain precision modeling of initial photon-induced interactions in ultra-peripheral collisions. They also provide a controllable baseline to search for possible final-state effects on lepton pairs resulting from the production of quark-gluon plasma in hadronic heavy ion collisions.”

<https://news.rice.edu/2021/09/20/physicists-probe-light-smashups-to-guide-future-research-2/>

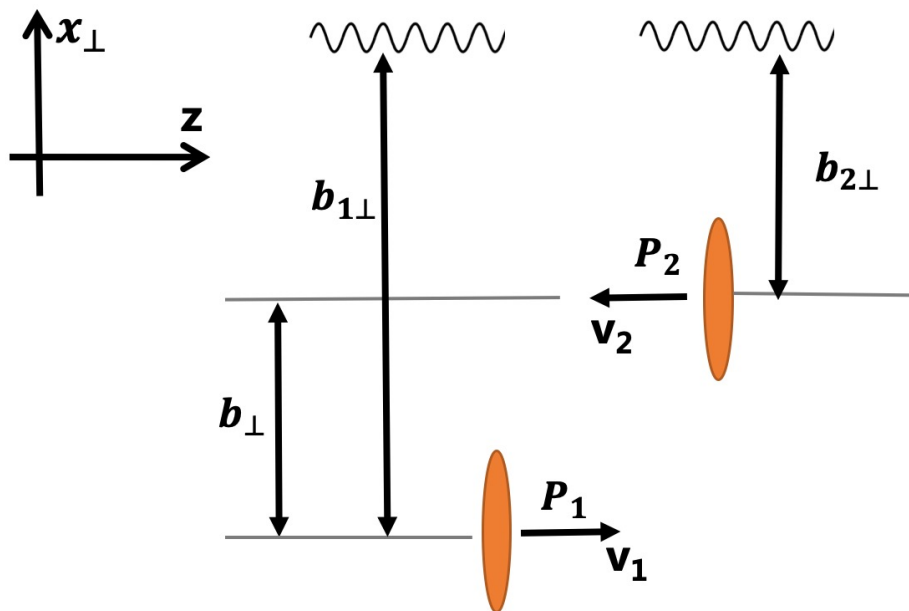


50. STAR Collaboration, J., Adam *et al.* Probing Extreme Electromagnetic Fields with the Breit-Wheeler Process. (2019). <https://arxiv.org/abs/1910.12400>.
51. ATLAS Collaboration. Measurement of non-exclusive dimuon pairs produced via  $\gamma\gamma$  scattering in Pb+Pb collisions at  $\sqrt{s_{NN}} = 5.02$  TeV with the ATLAS detector. ATLAS-CONF-2019-051. (2019). <https://inspirehep.net/literature/1762955>.
52. CMS Collaboration,. Observation of forward neutron multiplicity dependence of dimuon acoplanarity in ultra-peripheral PbPb collisions at  $\sqrt{s_{NN}} = 5.02$  TeV CMS-PAS-HIN-19-014. (2020). <https://inspirehep.net/literature/1798862>.



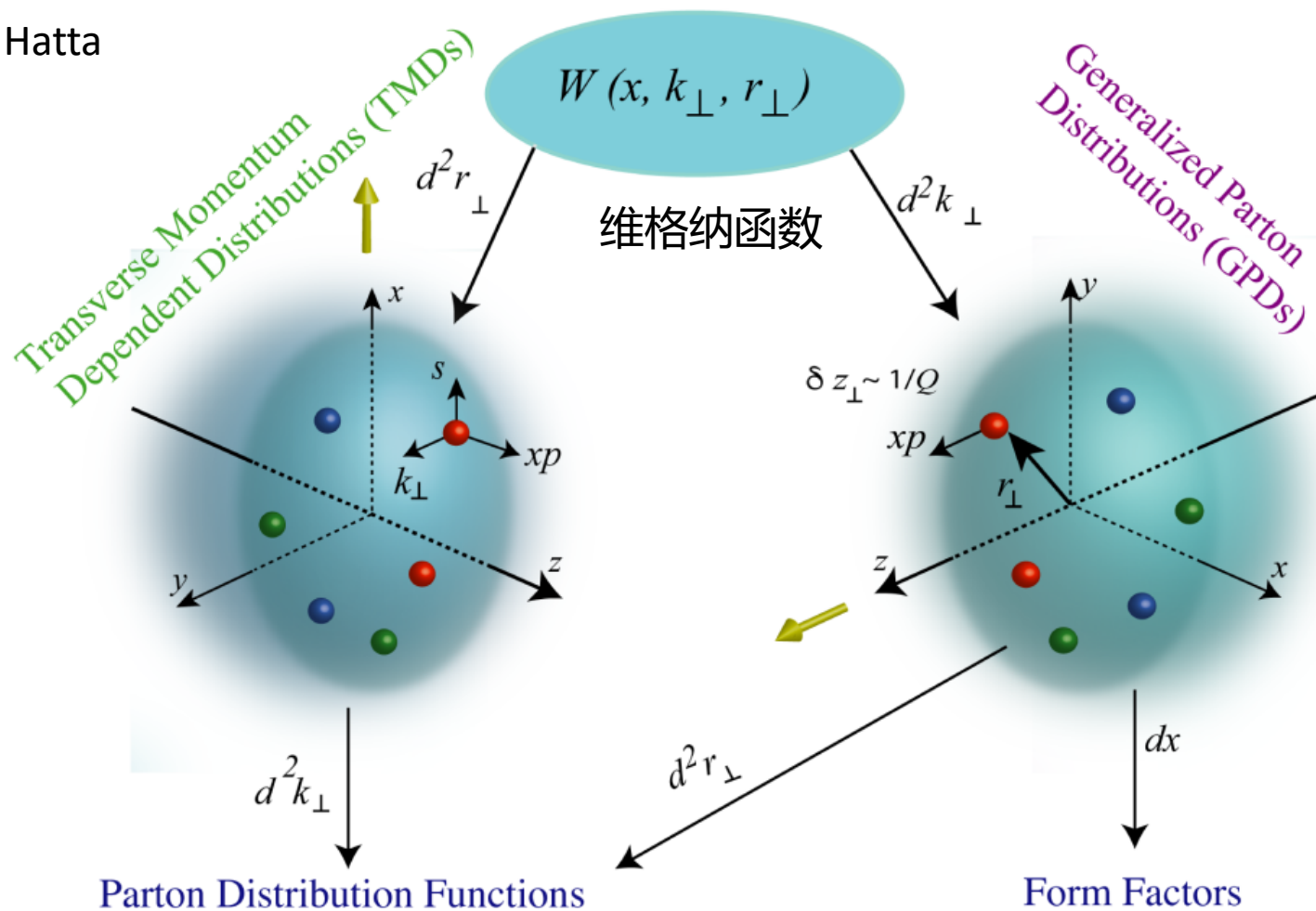
Quite a few techniques  
used in QCD  
can be used in  
strong-field QED as well

Understanding the QED is  
also important for  
quantitative extraction  
of the photoproduction



Y. Hatta

## Wigner Distributions



Wang/Pu/Wang, PRD, <https://arxiv.org/pdf/2106.05462.pdf>



# Lessons learned (AI↔Learning)

The simplest Equivalent Photon Approximation (EPA):

use photon-photon cross section

but ignore the interference of two LOQED diagrams,

integrate out the impact-parameter dependence,

Put back b-dependence by independently adding two-photon kinematics

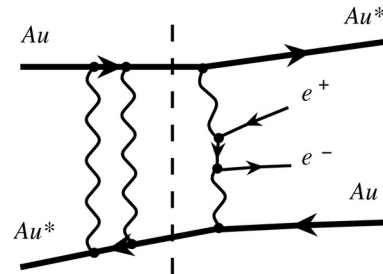
Last point use the Uncertainty Principle and produces the wrong conclusion.

## The reality:

LOQED is consistent with real photon approximation,

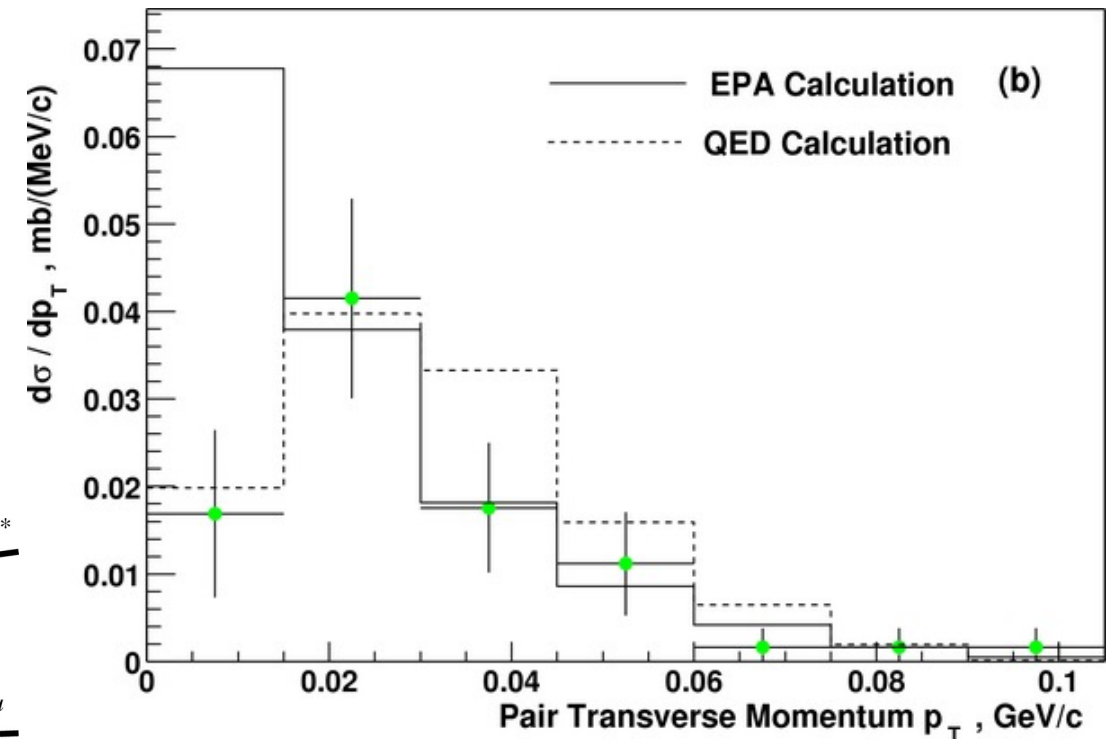
Photon momentum is correlated with position (Wigner function)

Interference and impact parameter should not be ignored.



STAR, Phys. Rev. C **70** (2004) 31902

Figure 2(b) shows the cross section as a function of pair  $p_T$ . The equivalent photon (solid) and QED (dashed) calculations differ when  $p_T < 15$  MeV/c, due to the nonzero photon virtuality in the QED calculation. The data agree with the QED calculation, but not with the equivalent photon calculation.



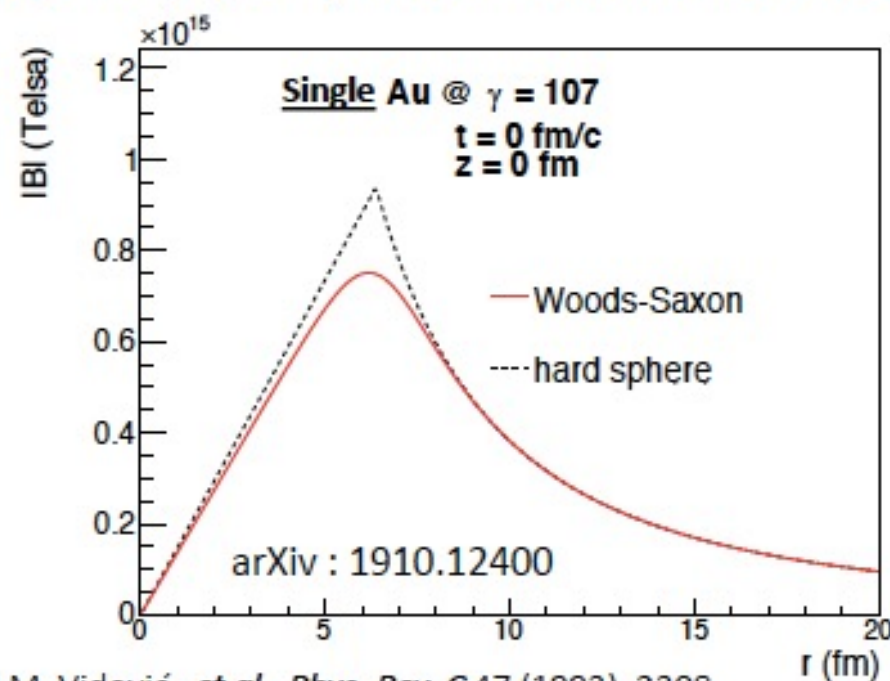
# Application : Mapping the Magnetic Field

Total and differential cross-sections (e.g.  $d\sigma/dP_{\perp}$ ) for  $\gamma\gamma \rightarrow e^+e^-$  are related to field strength and configuration

**photon density is related to energy flux of the electromagnetic fields [1]**

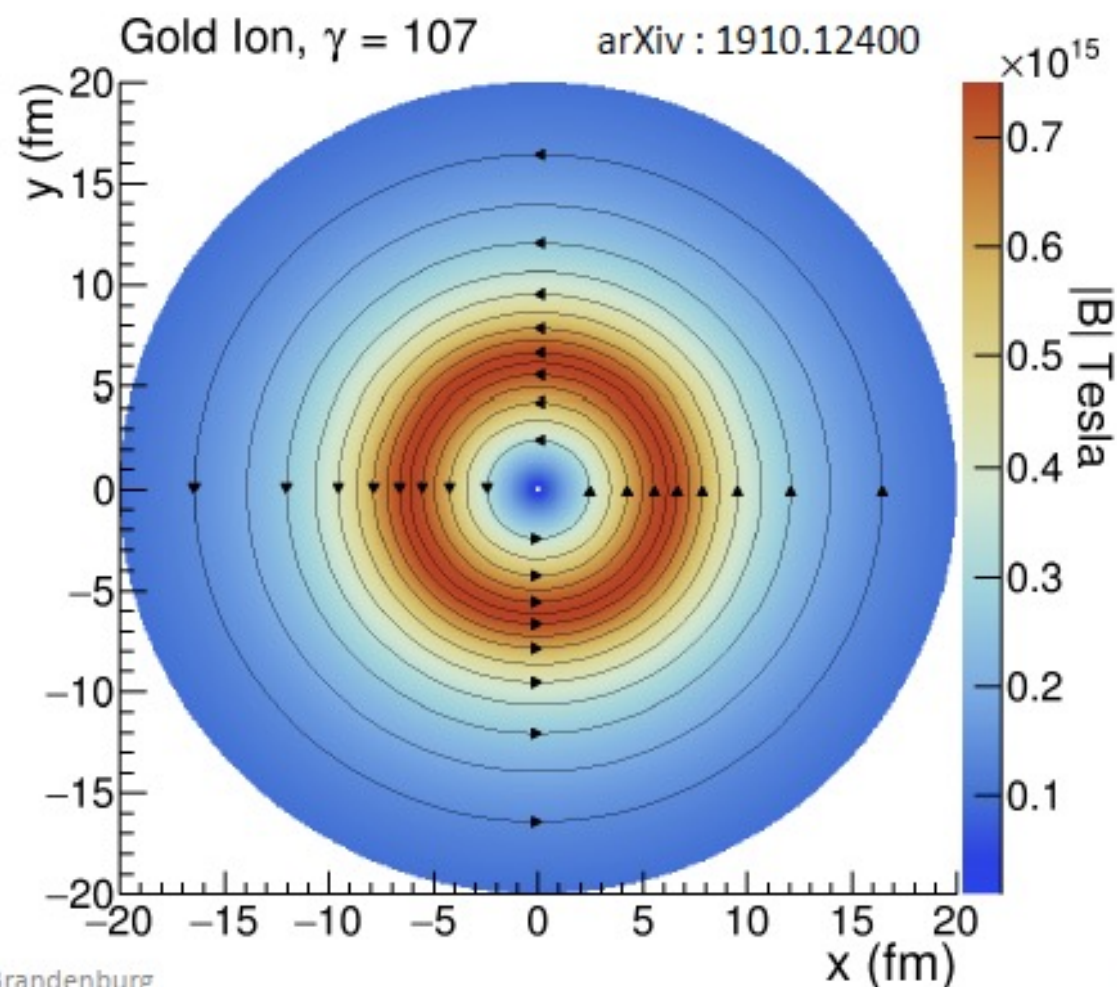
$$n \propto \vec{S} = \frac{1}{\mu_0} \vec{E} \times \vec{B}$$

→ Report  $\vec{B}$  (single ion) that matches measured cross-section



[1] M. Vidović, et al., Phys. Rev. C 47 (1993), 2308

11/05/19



Daniel Brandenburg

14



# Nuclear Radius Comparison

[1] STAR Collaboration, L. Adamczyk, *et al.*, *Phys. Rev. C* 96, 054904 (2017).  
 [2] H. Alvensleben, *et al.*, *Phys. Rev. Lett.* 24, 786 (1970).  
 [3] G. McClellan, *et al.*, *Phys. Rev. D* 4, 2683 (1971).



	Au+Au (fm)	U+U (fm)
Charge Radius	6.38 (long: 6.58, short: 6.05 )	6.81 (long: 8.01, short: 6.23)
Inclusive  t  slope (STAR 2017) [1]	$7.95 \pm 0.03$	--
Inclusive  t  slope (WSFF fit)*	$7.47 \pm 0.03$	$7.98 \pm 0.03$
Tomographic technique*	$6.53 \pm 0.03$ (stat.) $\pm 0.05$ (syst.)	$7.29 \pm 0.06$ (stat.) $\pm 0.05$ (syst.)
DESY [2]	$6.45 \pm 0.27$	$6.90 \pm 0.14$
Cornell [3]	$6.74 \pm 0.06$	--
Neutron Skin (Tomographic Technique)	$0.09 \pm 0.02$ (stat.) $\pm 0.05$ (syst.)	$0.41 \pm 0.03$ (stat.) $\pm 0.05$ (syst.) (Note: for Pb $\approx 0.3$ )

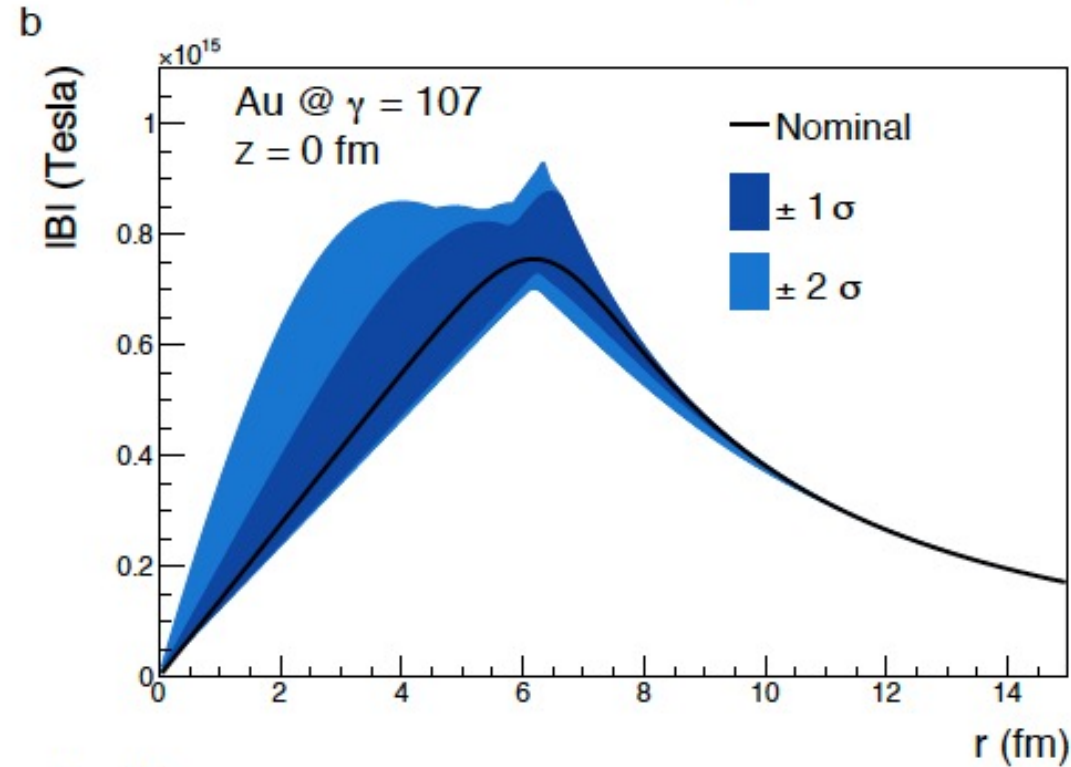
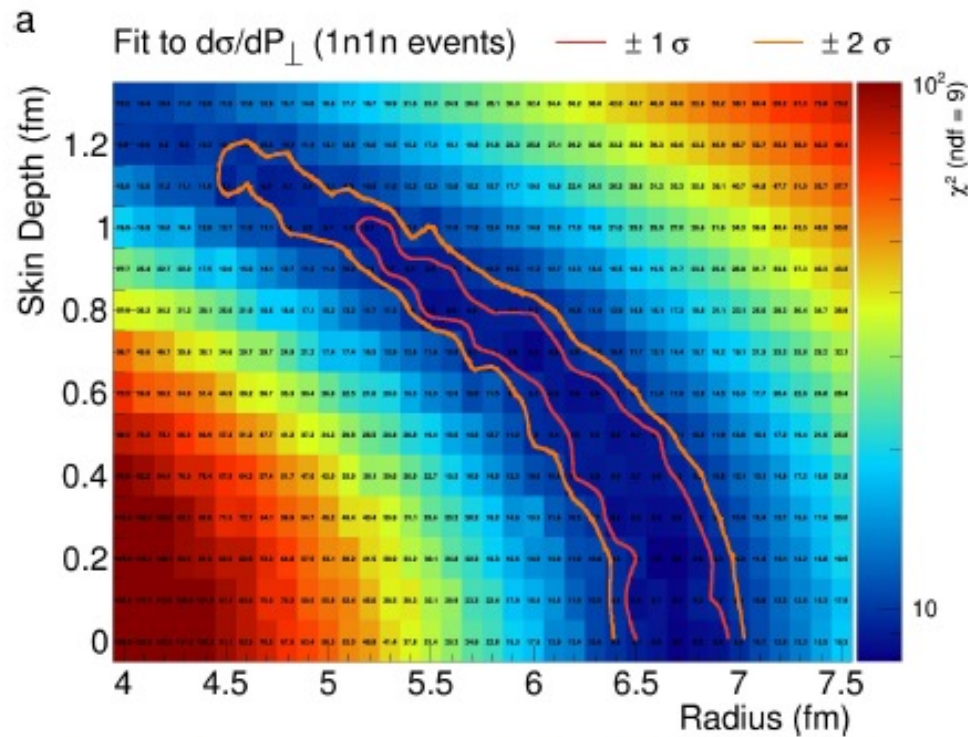
\*STAR Preliminary

**Precision measurement of nuclear interaction radius at high-energy**  
**Measured radius of Uranium shows evidence of (relatively) large neutron skin**

# Mapping of EM Field Distribution

STAR, arXiv : 1910.12400  
JDB, W Zha, Z Xu, arXiv:2103.16623

Precision transverse momentum + polarization = constrain field spatial extent

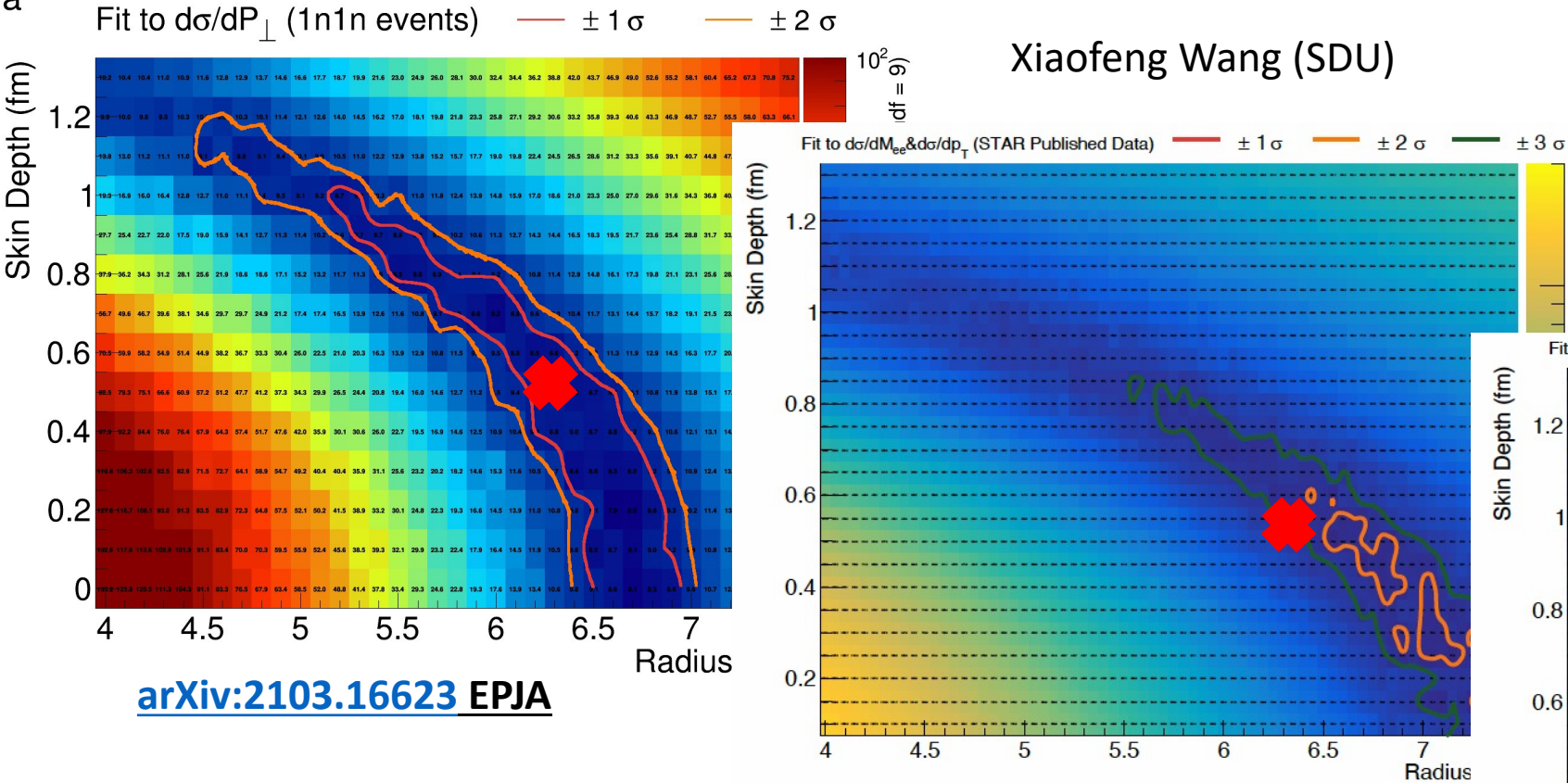


- Much stronger field possible at small distances
  - More measurements needed to constrain event-by-event fluctuations of EM fields
- **Novel input for magnetic-field driven phenomena**



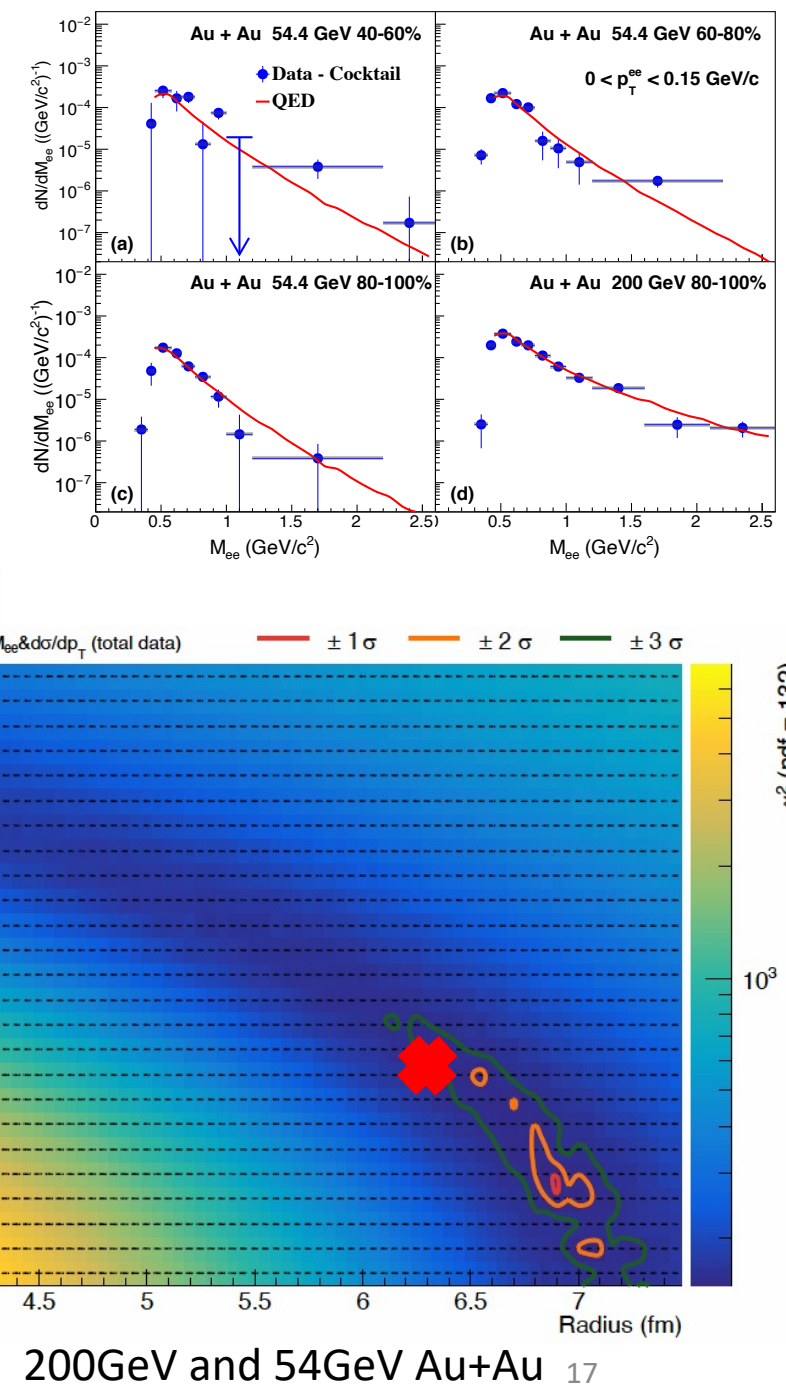
# Constraint on charge distribution with precision

a



Low energy scattering:  $R=6.38\text{fm}$ ,  $d=0.535\text{fm}$

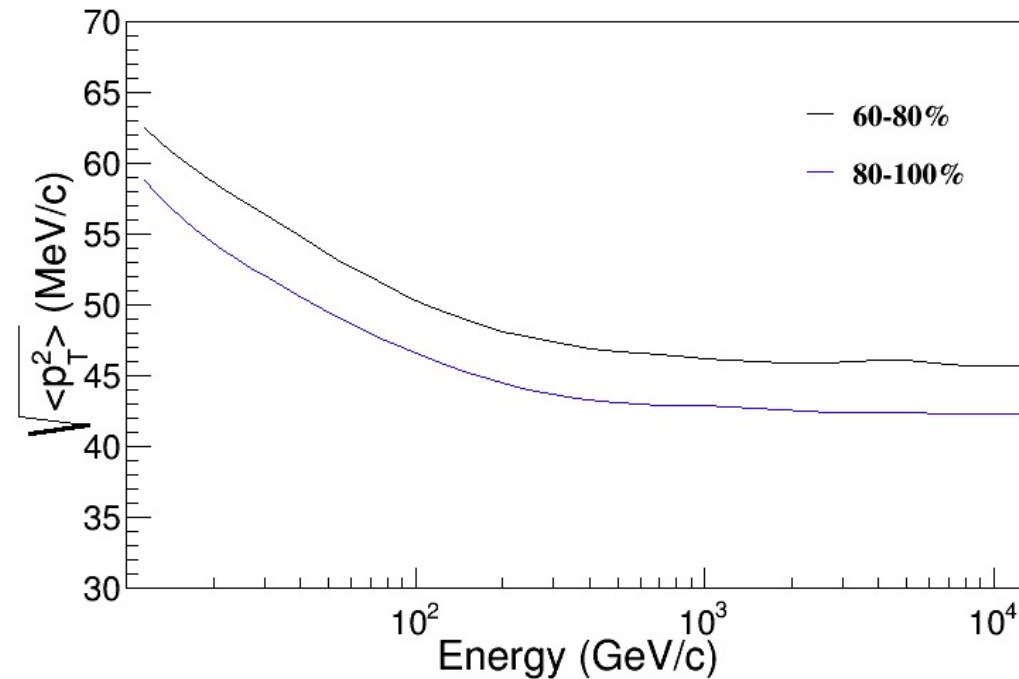
Use WS distribution and output to obtain best  $\chi^2$  to the data points  
A hint of sharper distribution (larger radius and smaller skin)



# Energy-dependence measurements sensitive to the infrared-divergence term

- QED has a well-known infrared-divergence due to the massless of photons ( $1/q^4$ )  
In e+e- collisions, the interaction can be formulated as photon collisions with finite momentum transfer (virtuality) cutoff:  $q_{\min}$  and  $q_{\max}$  since  $\gamma \rightarrow \infty$   
(particle data group 2020, section 50.7 Eq.50.44)
- Heavy-ion UPC at RHIC naturally regulated by the form factor at high  $q$  and finite  $\omega/\gamma$  at low  $q$ . This is crucial for discovery of the Breit-Wheeler process and the photon spatial-momentum-spin correlation  
**Vector direction and resolving power become poor as  $q \rightarrow 0$**
- We can further test this by studying the beam energy ( $\gamma$ ) dependence of  $\langle p_t \rangle$ . Analytic integration:  
$$\langle p_t^2 \rangle = \int_0 p_t^2 dn \approx (\hbar/R)^2 - 4 \left( \frac{\omega}{\gamma} \right)^2 \ln \left( \frac{R\omega}{\gamma} \right)$$
  
For  $\omega=300\text{MeV}$ ,  $R=6.8\text{fm}$ ,  
BW  $\langle p_t \rangle \approx 41\text{MeV}$  at  $\gamma \rightarrow \infty$ ,  $44\text{MeV}$  at  $\gamma=100$ ,  $53\text{MeV}$  at  $\gamma=25$ ;

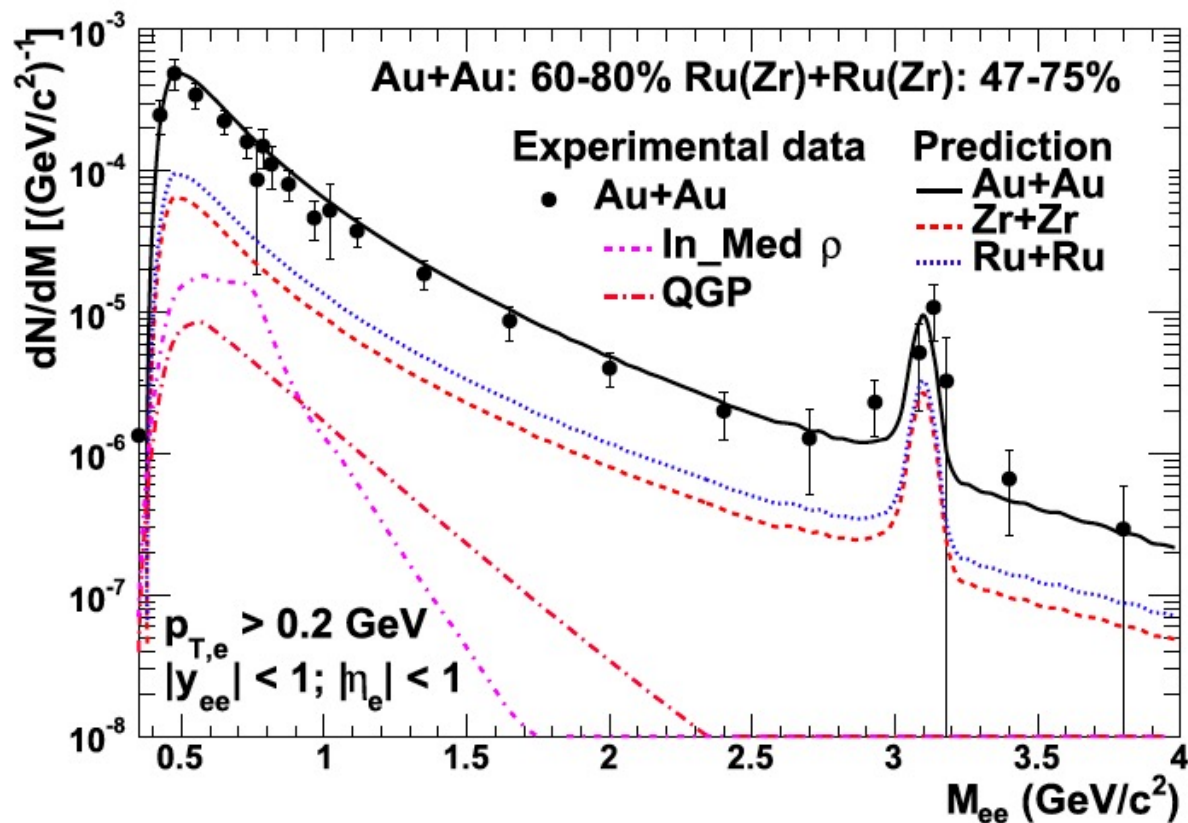
$$dn_i = \frac{Z_i^2 \alpha}{\pi^2} \frac{q_{i\perp}^2 \left[ F \left( q_{i\perp}^2 + \frac{w_i^2}{\gamma^2} \right) \right]^2}{\left( q_{i\perp}^2 + \frac{w_i^2}{\gamma^2} \right)^2} \frac{d^3 q_i}{w_i}$$



X.F. Wang (SDU)



# Isobar data on charge distribution



STAR 2017 BUR

Physics process	47-75% Zr+Zr (data/cocktail)	47-75% Ru+Ru (data/cocktail)	Difference between Zr+Zr and Ru+Ru
Photonuclear	$14.3 \pm 0.4$	$16.1 \pm 0.4$	$1.8 \pm 0.6 \text{ (3.0 } \sigma)$
Two-photon	$14.2 \pm 0.4$	$17.4 \pm 0.4$	$3.2 \pm 0.6 \text{ (5.3 } \sigma)$

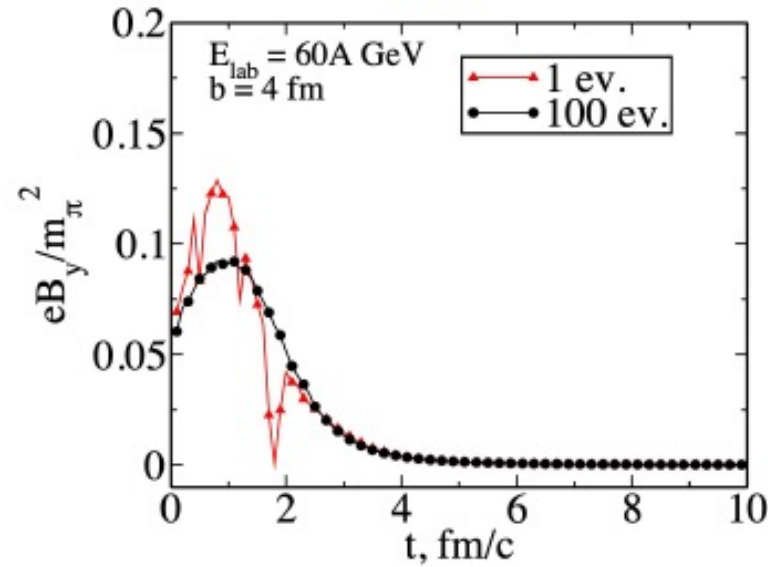
Table 5.3: The expected di-electron data over cocktail ratios in the mass region  $0.4\text{-}0.76 \text{ GeV/c}^2$  for  $p_T < 0.15 \text{ GeV/c}$  with 1.2 billion minimum-bias isobar collisions and the projected differences for the two physics scenarios in Zr+Zr and Ru+Ru collisions.

Physics process	47-75% Zr+Zr (data/cocktail)	47-75% Ru+Ru (data/cocktail)	Differences between Zr+Zr and Ru+Ru
Photonuclear	$17.5 \pm 1.7$	$20.0 \pm 1.7$	$2.5 \pm 2.4 \text{ (1.0 } \sigma)$
Two-photon	$17.3 \pm 1.7$	$21.8 \pm 1.7$	$4.5 \pm 2.4 \text{ (1.9 } \sigma)$

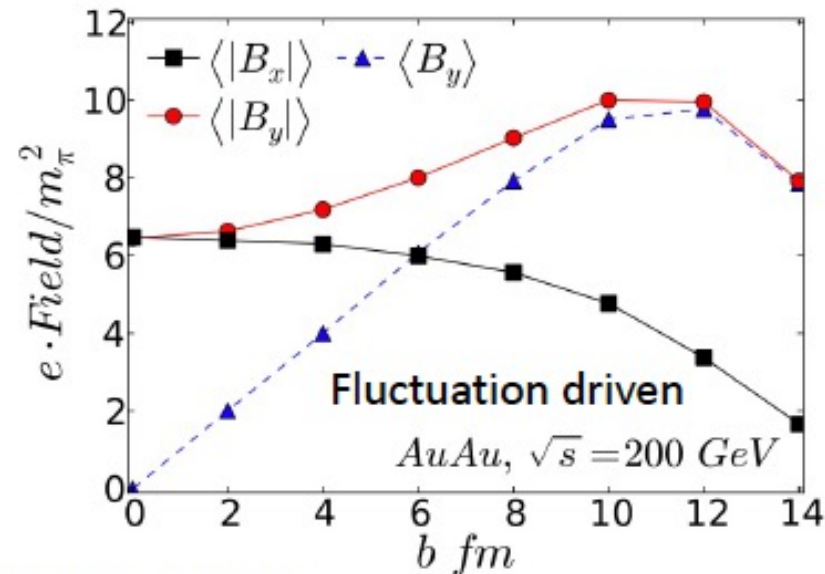
Table 5.4: The expected di-electron data over cocktail ratios in the mass region  $3.0\text{-}3.2 \text{ GeV/c}^2$  for  $p_T < 0.15 \text{ GeV/c}$  with 1.2 billion minimum-bias isobar collisions and the projected differences for the two physics scenarios in Zr+Zr and Ru+Ru collisions.

Expected data: x3 more data than used in BUR  
 J/Psi trigger data in addition

# Searching for Medium Effects

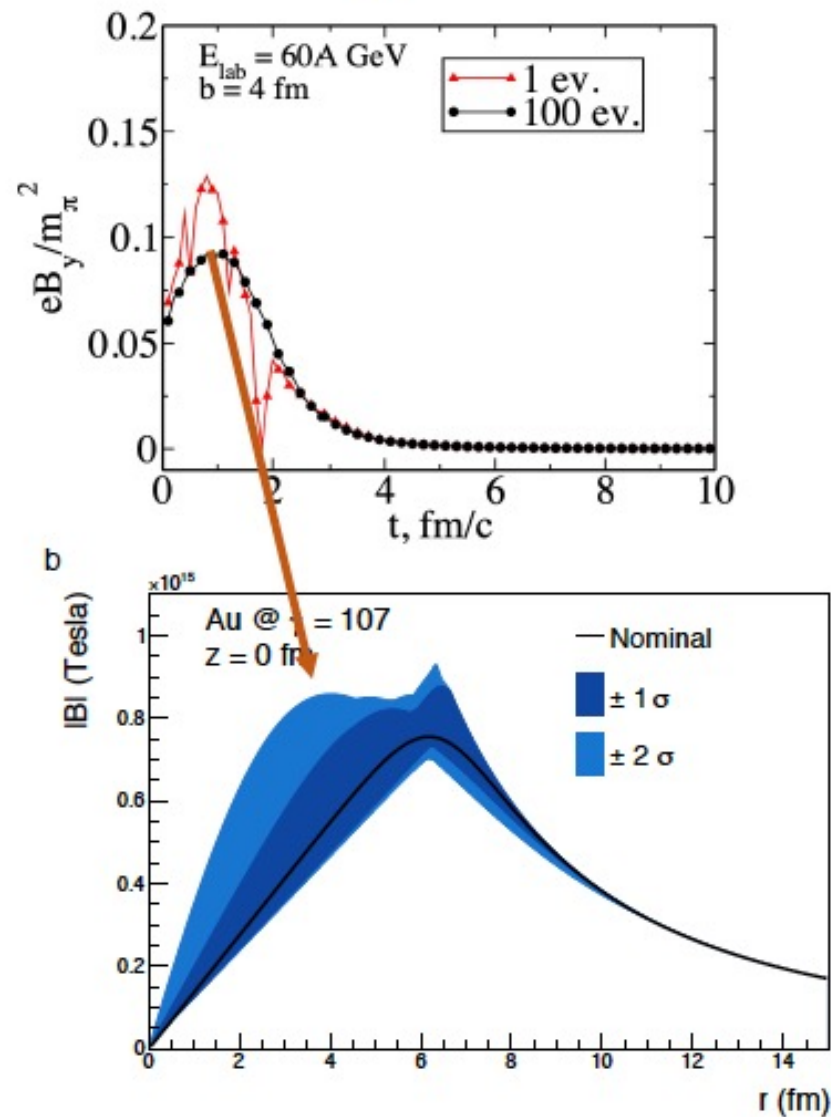


- Question:
  - Field at low-x and effect of event-by-event fluctuations
- Possible Effect:
  - Modified  $P_\perp$  and  $\alpha$  distribution
  - Modification of relative photon-photon polarization angle  
→ Modified  $\cos 4\phi$  modulation



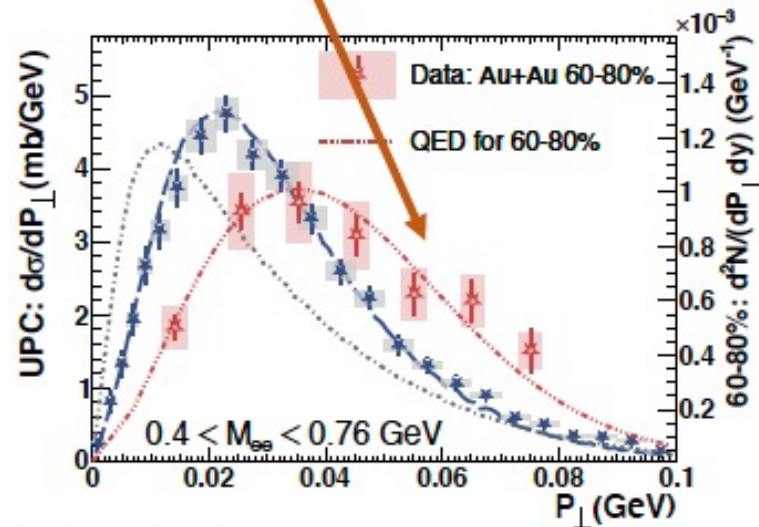
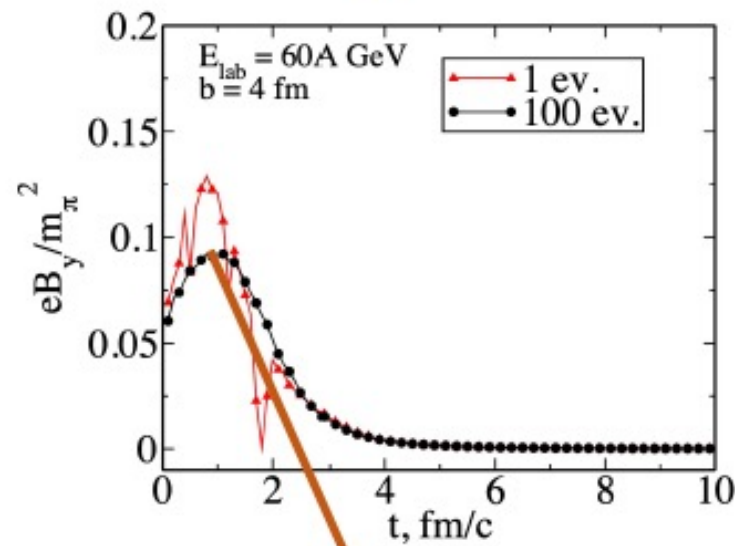


# Event-by-event Fluctuations + Interactions



- Significantly stronger field possible at small radial distances (based on current data)
- Fluctuating nucleon positions effect field inside nucleus
- OR Long-lived magnetic field  
→ Lorentz-force bending of pairs
- High precision data from STAR 2023-25
- What to look for:
  - Field at small distance → large  $P_\perp$  and  $\alpha$
  - Look for modification of  $d\sigma/dP_\perp$  shape

# Event-by-event Fluctuations + Interactions



- Significantly stronger field possible at small radial distances (based on current data)
- Fluctuating nucleon positions effect field inside nucleus
- OR Long-lived magnetic field  
→ Lorentz-force bending of pairs
- High precision data from STAR 2023-25
- What to look for:
  - Field at small distance → large  $P_\perp$  and  $\alpha$
  - Look for modification of  $d\sigma/dP_\perp$  shape

Hint of modification in 60 – 80% central collisions:

**Additional  $14 \pm 4$  (stat.)  $\pm 4$  (syst.) MeV/c broadening**



# Are there final-state QED effects?

Precision data with  
QED theory comparisons:  
Both on-going at LHC and RHIC

How about azimuthal anisotropy  
relative to reaction plane?

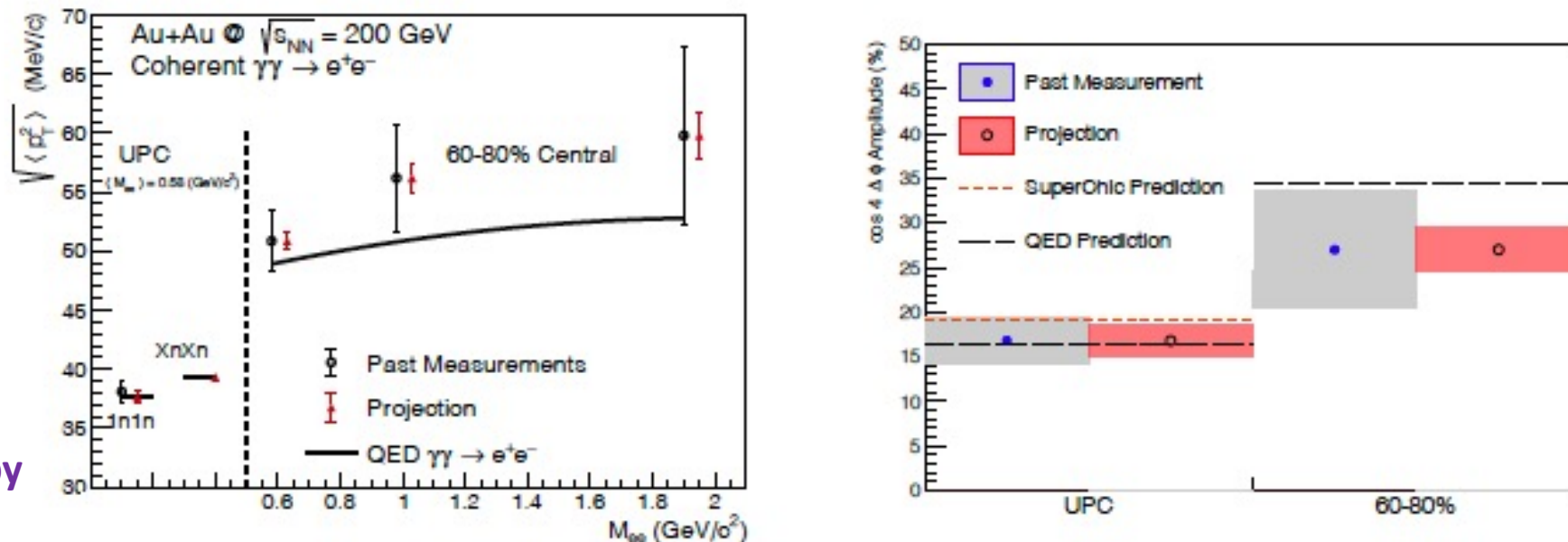


**Figure 57:** (Color online) Projections for measurements of the  $\gamma\gamma \rightarrow e^+e^-$  process in peripheral and ultra-peripheral collisions. Left: The  $\sqrt{\langle p_T^2 \rangle}$  of di-electron pairs within the fiducial acceptance as a function of pair mass,  $M_{ee}$ , for 60–80% central and ultra-peripheral Au+Au collisions at  $\sqrt{s_{NN}} = 200$  GeV. Right: The projection of the  $\cos 4\Delta\phi$  measurement for both peripheral (60–80%) and ultra-peripheral collisions.

STAR Beam Use Request (2023-2025):

[https://drupal.star.bnl.gov/STAR/system/files/BUR2020\\_final.pdf](https://drupal.star.bnl.gov/STAR/system/files/BUR2020_final.pdf)

$p_T$  broadening and azimuthal correlations of  $e^+e^-$  pairs sensitive to electro-magnetic (EM) field;  
Impact parameter dependence of transverse momentum distribution of EM production is the key component to describe data.

Is there a sensitivity to final magnetic field in QGP?

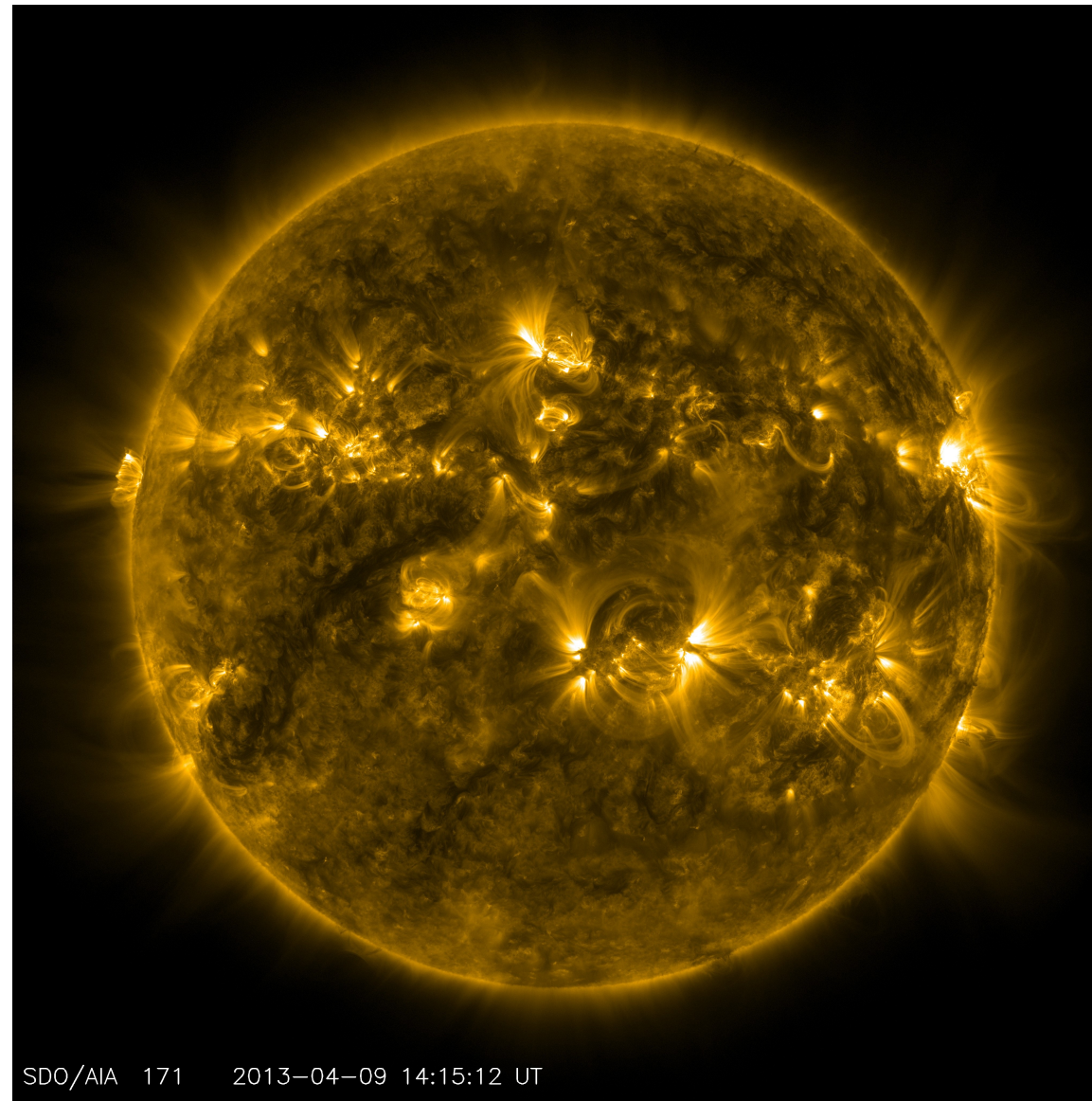
Precise measurement of  $p_T$  broadening and angular correlation will tell at  $>3\sigma$  for each observable.



# Best example of magnetohydrodynamics: SUN

**Magnetohydrodynamics (MHD)** is the study of the magnetic properties and behavior of electrically conducting fluids. Examples of such magnetofluids include plasmas, liquid metals, salt water, and electrolytes. The word "magnetohydrodynamics" is derived from *magneto*-meaning magnetic field, *hydro*-meaning water, and *dynamics* meaning movement. The field of MHD was initiated by Hannes Alfvén, for which he received the Nobel Prize in Physics in 1970. The fundamental concept behind MHD is that magnetic fields can induce currents in a moving conductive fluid, which in turn polarizes the fluid and reciprocally changes the magnetic field itself. The set of equations that describe MHD are a combination of the Navier–Stokes equations of fluid dynamics and Maxwell's equations of electromagnetism. These differential equations must be solved simultaneously, either analytically or numerically.

Wikipedia



磁流体动力学

QED+QCD?

This image taken by the Solar Dynamics Observatory's Atmospheric Imaging Assembly (AIA) instrument at 171 Angstrom shows the current conditions of the quiet corona and upper transition region of the Sun.

*Image Credit: NASA/SDO  
Last Updated: Aug. 7, 2017  
Editor: NASA Content Administrator*

# Summary

- Data show clearly sensitivity to the nuclear charge geometry
- Need model and data comparison to extract nuclear radius
- Current study of Breit-Wheeler process and vector-meson diffractive shows
  - Consistence between charge radius at low energy and RHIC
  - large difference between charge radius and strong-interaction radius in Uranium
- High-statistics in future will be able to probe final-state EM effect in QGP
- Isobar data with BW  $e^+e^-$  can be used to determine the EM field difference and if there is final-state effect

# Charge vs baryon stopping and how isobar data can help

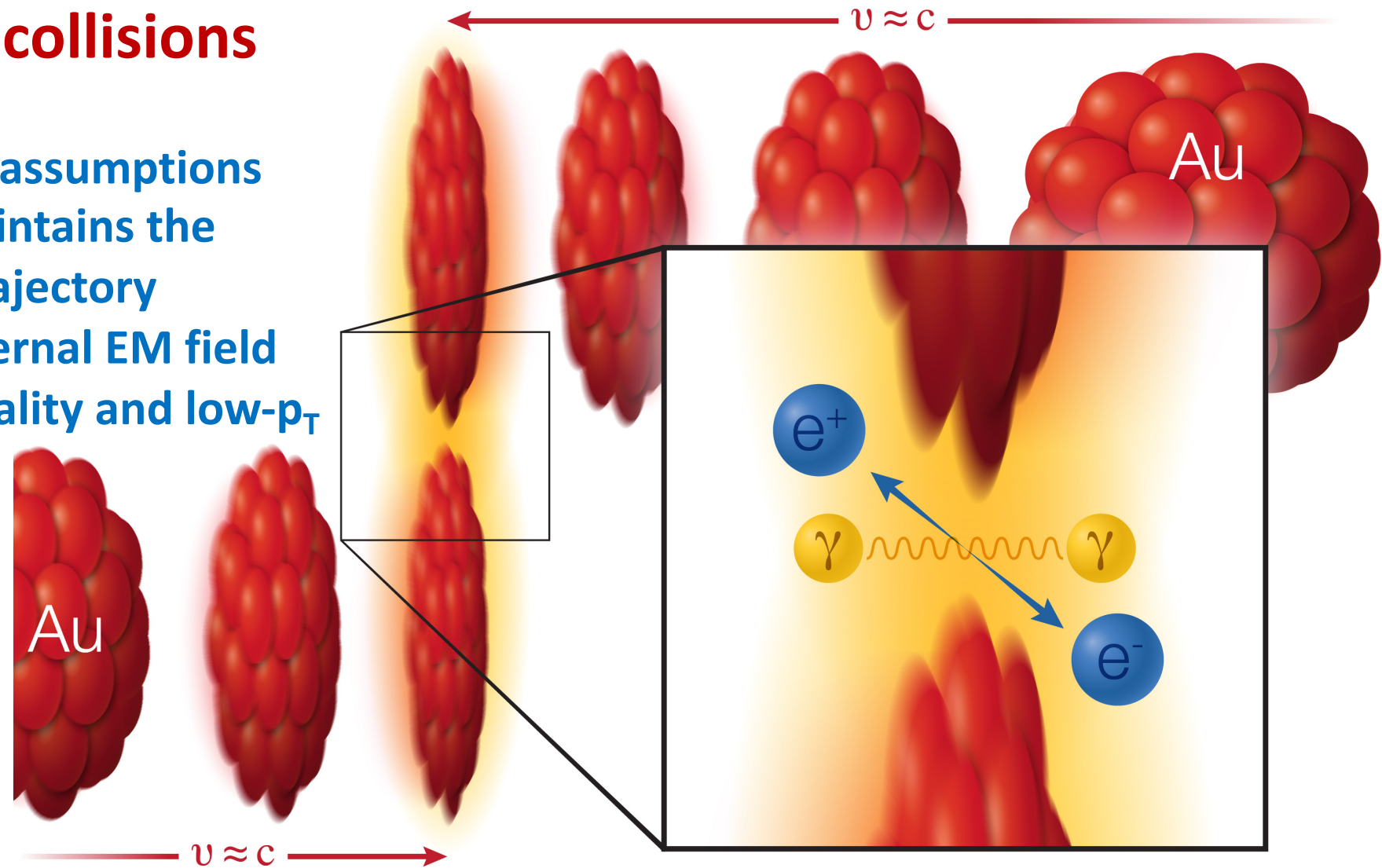
- BES-Tea Seminar:
- [https://drive.google.com/file/d/12wis6PcofzqF6q0Smb\\_E0W2TFmIcVSk1/view](https://drive.google.com/file/d/12wis6PcofzqF6q0Smb_E0W2TFmIcVSk1/view)



# UPC AND peripheral collisions

One of the most important assumptions is that the ions (charge) maintains the velocity and straight-line trajectory

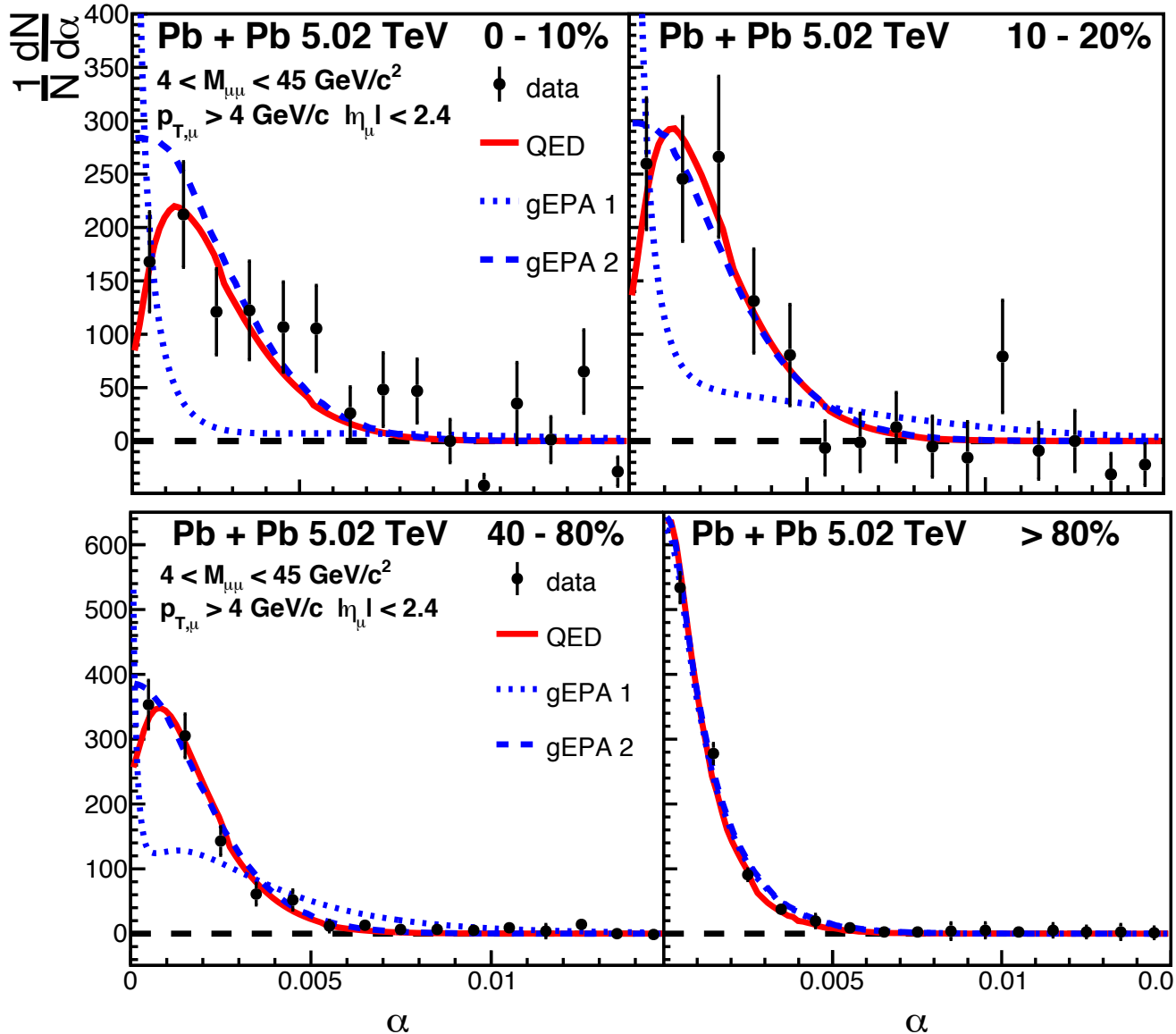
One can then quantize external EM field as photons with small virtuality and low- $p_T$



Two gold (Au) ions (red) move in opposite direction at 99.995% of the speed of light ( $v$ , for velocity, = approximately  $c$ , the speed of light). As the ions pass one another without colliding, two photons ( $\gamma$ ) from the electromagnetic cloud surrounding the ions can interact with each other to create a matter-antimatter pair: an electron ( $e^-$ ) and positron ( $e^+$ ).

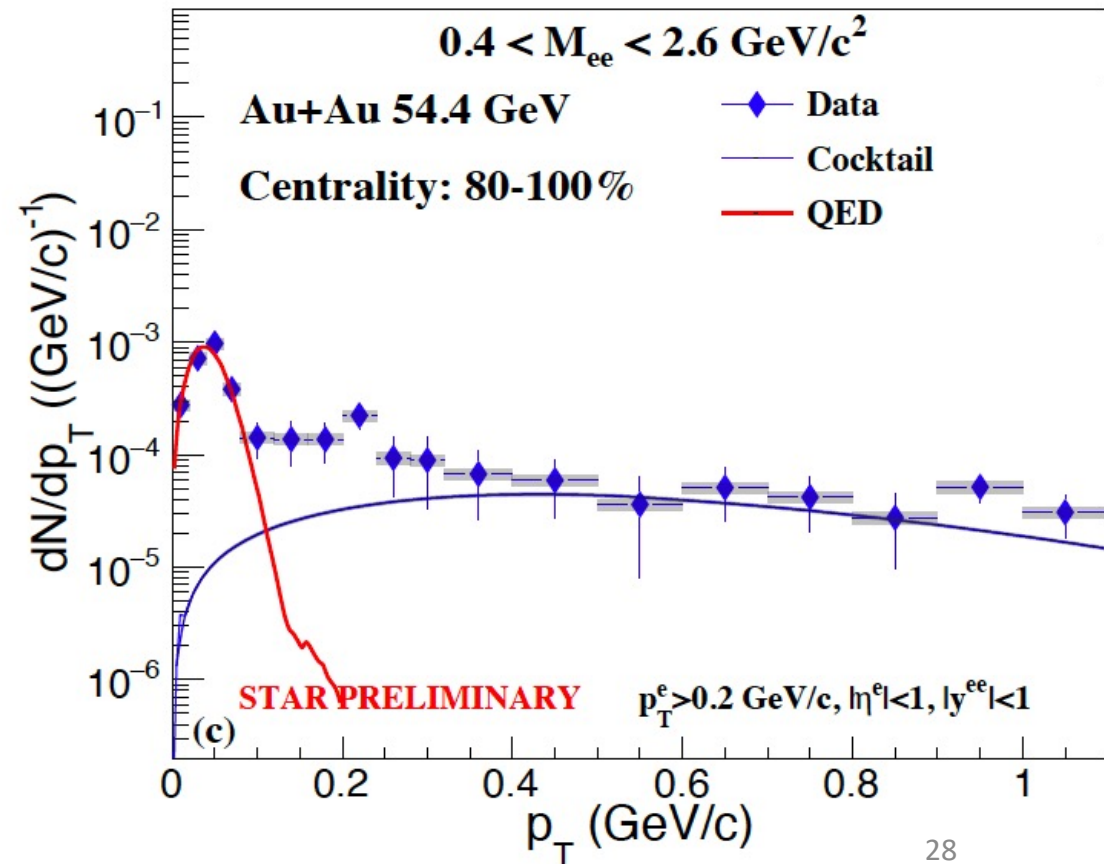
# Other RHIC and LHC energies and centralities

ATLAS data: PRL 121 (2018) 212301



If straight-line and velocity of charges do not maintain, there is not reason to have low-pt,  $\cos(4\phi)$  and cross section as predicted by QED which assumes those And the J/Psi photoproduction ...

Xiaofeng Wang for STAR, IS 2021

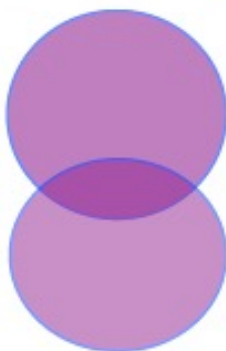




## Method III: net-charge ratio in very peripheral collisions

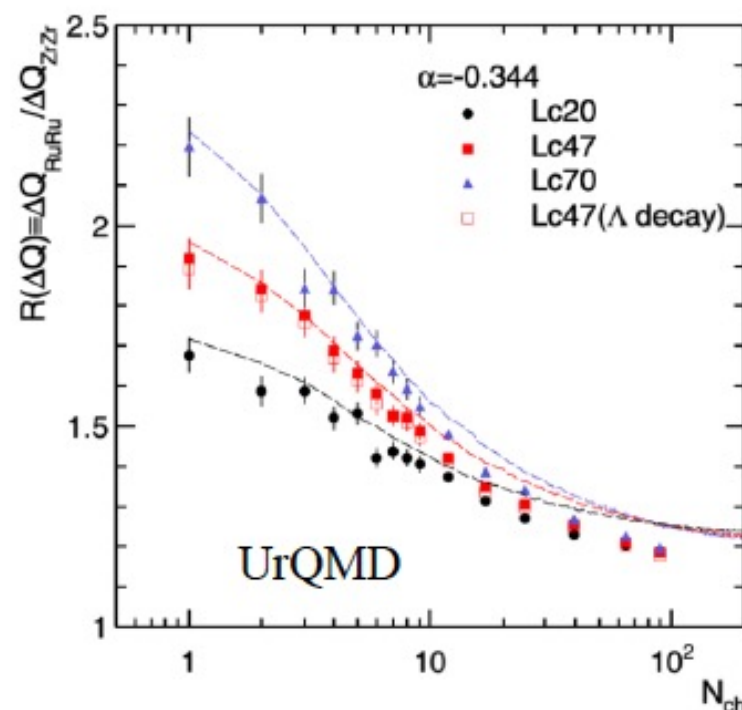
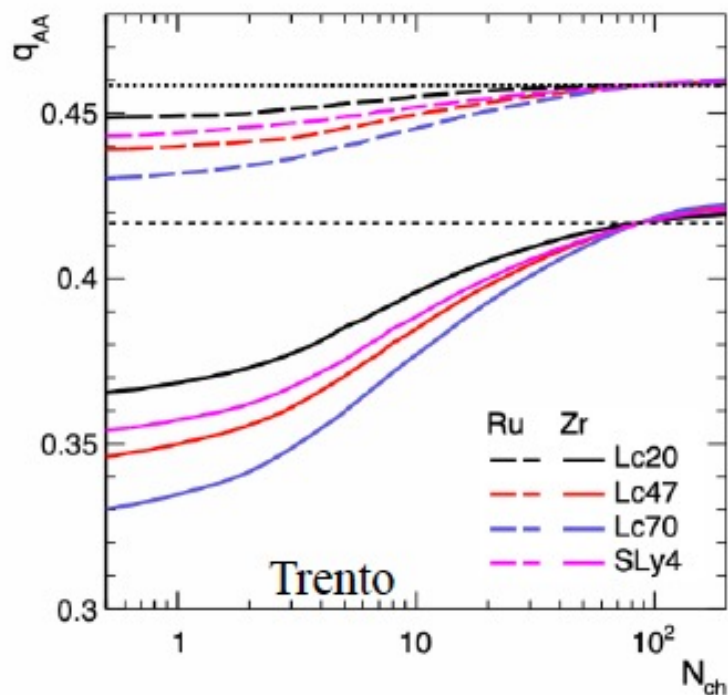
HJX, et.al., PRC105, L011901 (2022)

For the colliding nuclei with large neutron skin thickness



more n+n collisions at most peripheral collisions

Less participant charges, thus less final net-charges



The curves are calculated by superimposition assumption

$$R(\Delta Q) = \frac{q_{RuRu} + \alpha / (1 - \alpha)}{q_{ZrZr} + \alpha / (1 - \alpha)}$$

where  $q_{RuRu/ZrZr}$  are the fraction of protons among the participant nucleons, obtained by the Trento model.

$\alpha$  is the  $\Delta Q$  ratio in nn to pp interaction:

Pytha:  $\alpha = -0.352$

Hijing:  $\alpha = -0.389$

UrQMD:  $\alpha = -0.344$



# Baryon Junction

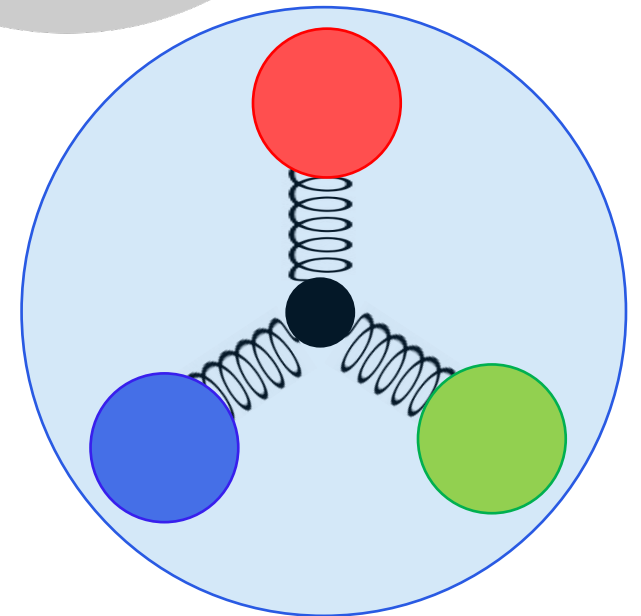
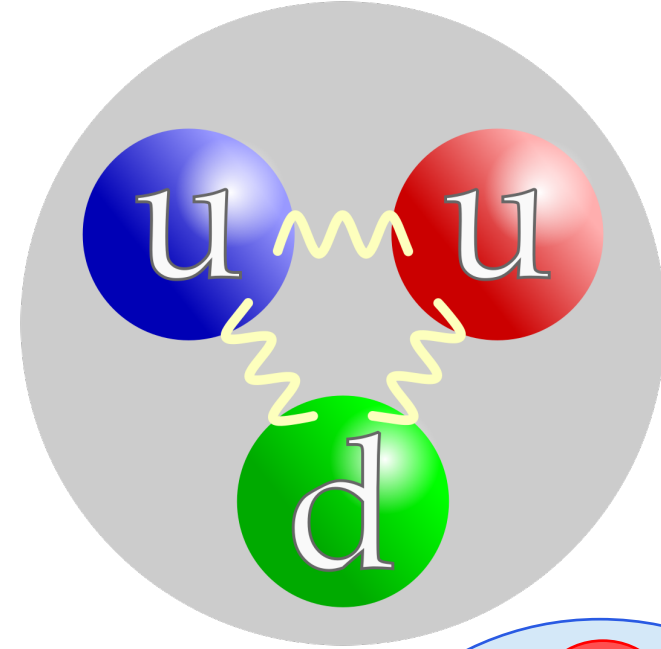
- Many of the models used for heavy-ion collisions at RHIC (HIJING, AMPT, UrQMD) have implemented a nonperturbative baryon stopping mechanism

V. Topor Pop, *et al*, Phys. Rev. C **70**, 064906 (2004)

Zi-Wei Lin, *et al*, Phys. Rev. C **72**, 064901 (2005)

M. Bleicher, *et al*, J.Phys.G **25**, 1859-1896 (1999)

- Baryon Junction: nonperturbative configuration of gluons linked to all three valence quarks
  - Carries the baryon number
  - Theorized to be an effective mechanism of stopping baryons in  $pp$  and  $AA$
- D. Kharzeev, Physics Letters B **378**, 238-246 (1996)
- But no signature of baryon junction has been cleanly identified in the experiment



# Model implementations of baryons at RHIC

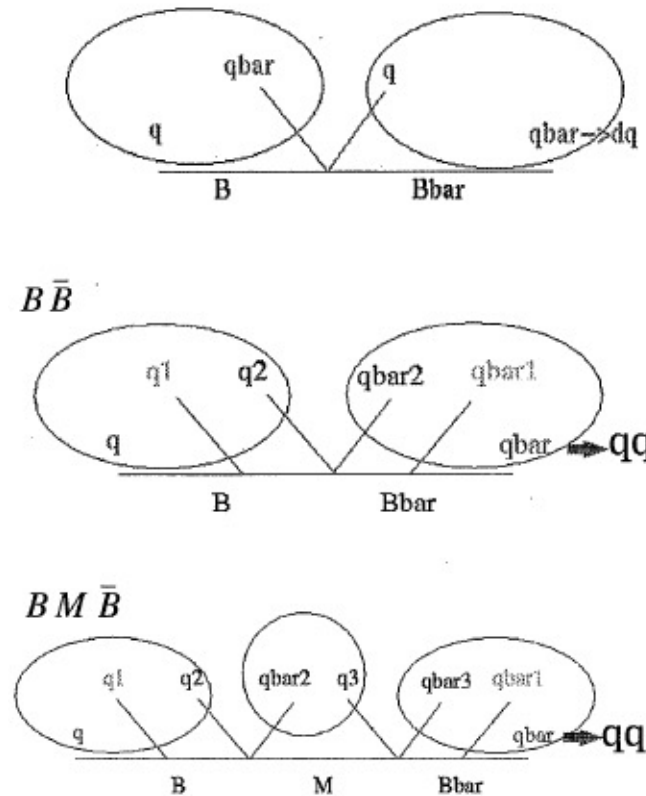
## HIJING/B $\bar{B}$ v 1.10 Outline

Experimental data at CERN-SPS on p+A and A+B interactions has revealed a large degree of stopping and strange hyperon production in the heavy nuclear systems. The stopping is significantly under-predicted by models which assume that the primary mechanism for baryon transport is diquark-quark hadronic strings (Gyulassy, Topor, Vance, 97).

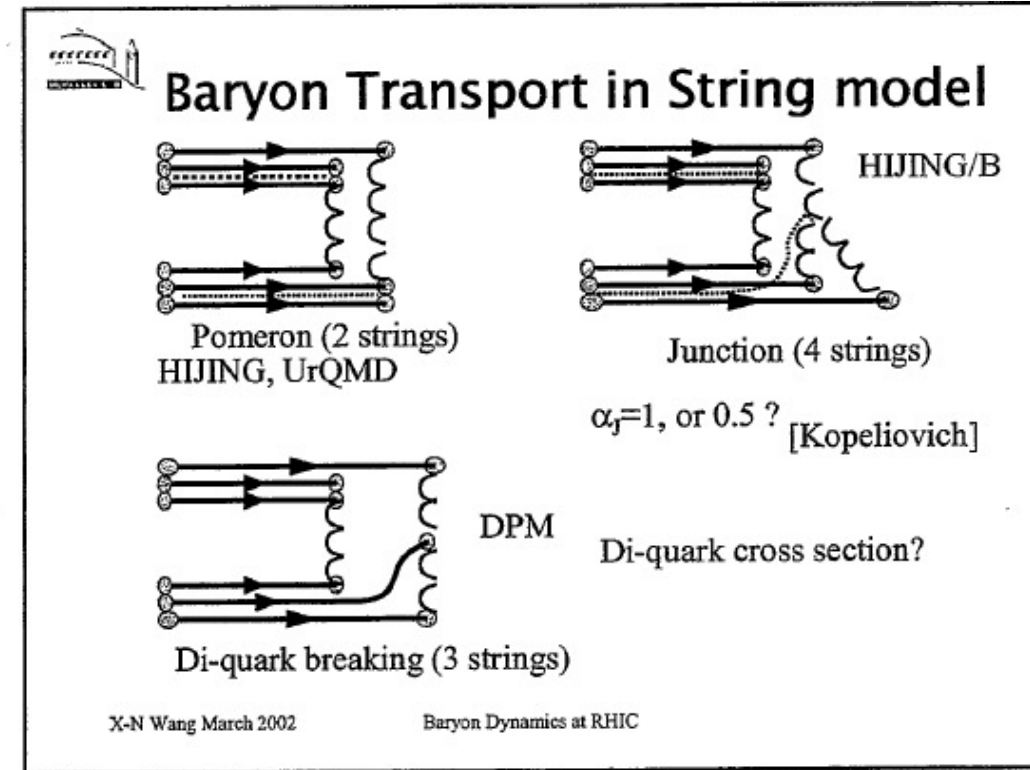
- Baryon junction mechanism, a novel non-equilibrium hadronic mechanism derived from the Y-shaped ( $SU_c(3)$ ) gluon structure of the baryon, has been introduced within HIJING/B to explain these observations. (Vance and Gyulassy, 98). **Abandoned?**
- The valence baryon junction exchange mechanism has been extended by including junction-antijunction ( $J\bar{J}$ ) loops that naturally arise in Regge phenomenology. HIJING/B $\bar{B}$  v1.10, (Vance, Gyulassy and Wang, 99) is now available.
- Fitting  $\bar{p}$  and  $\bar{\Lambda}$  data from p+p and p+S interactions, the cross section for  $J\bar{J}$  exchange is found to be  $\sigma_{B\bar{B}} = 6$  mb. The threshold cutoff mass  $m_c = 6$  GeV, provides sufficient kinematical phase space for fragmentation of the strings and for  $B\bar{B}$  pair production. This kinematic constraint severely limits the number of allowed  $J\bar{J}$  configurations, reducing its effective cross section to  $\approx 3$  mb. **at SPS.**

V. Topor Pop

With popcorn scheme:



Z.W. Lin (AMPT)



X.N. Wang (theory summary)

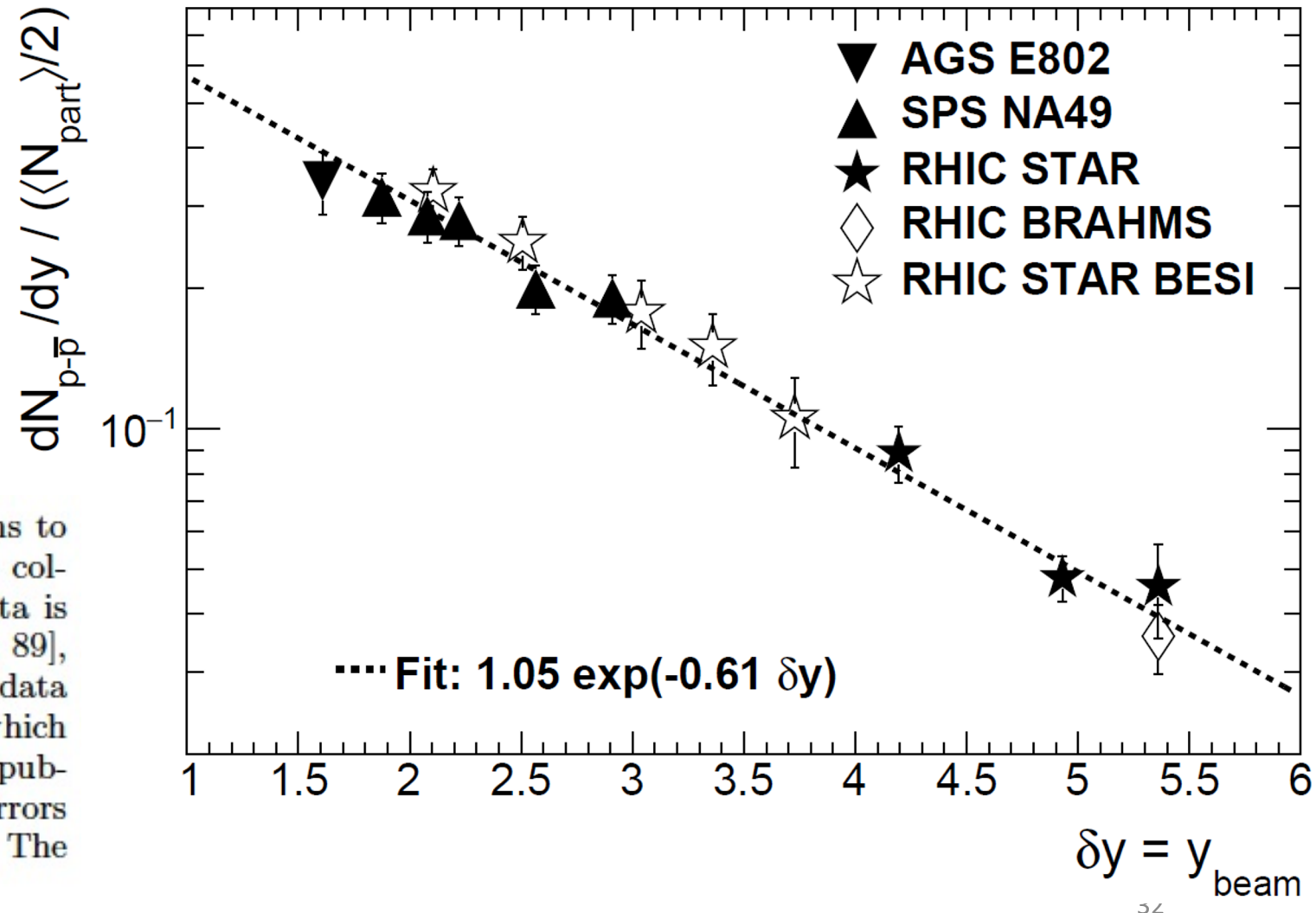
# Different ways of quantifying baryon rapidity loss

STAR, Phys. Rev. C 79 (2009) 34909; 96 (2017) 44904

Keep in mind that  
the exponential slope  
is close to  $\frac{1}{2}$

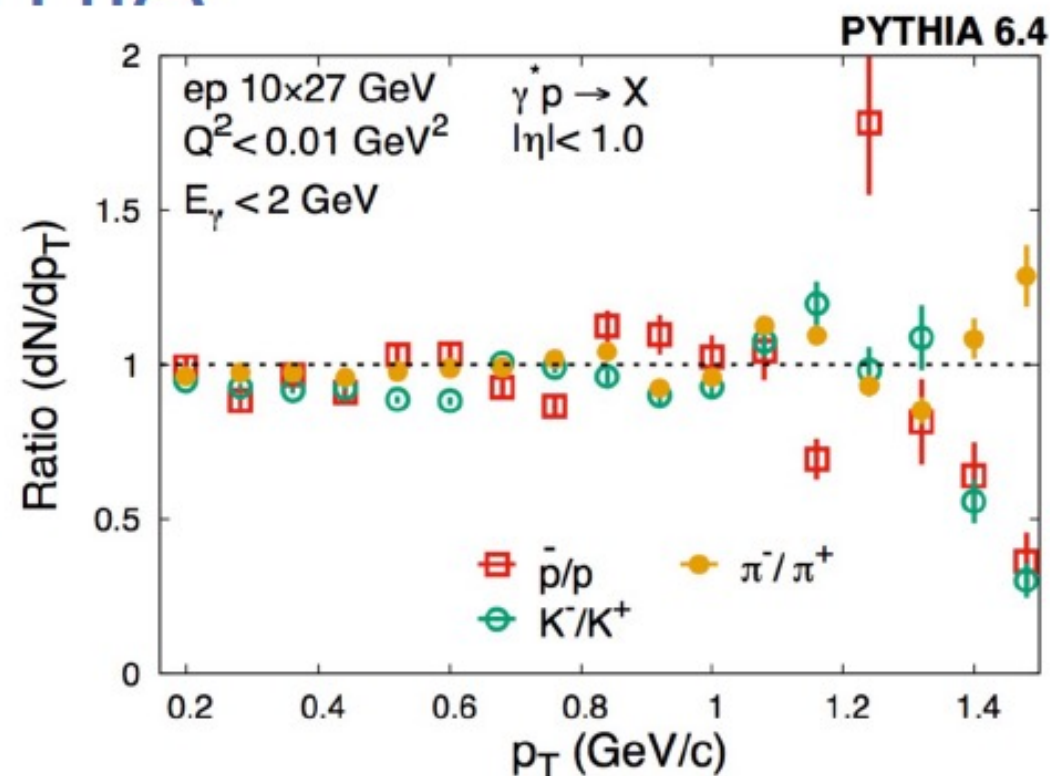
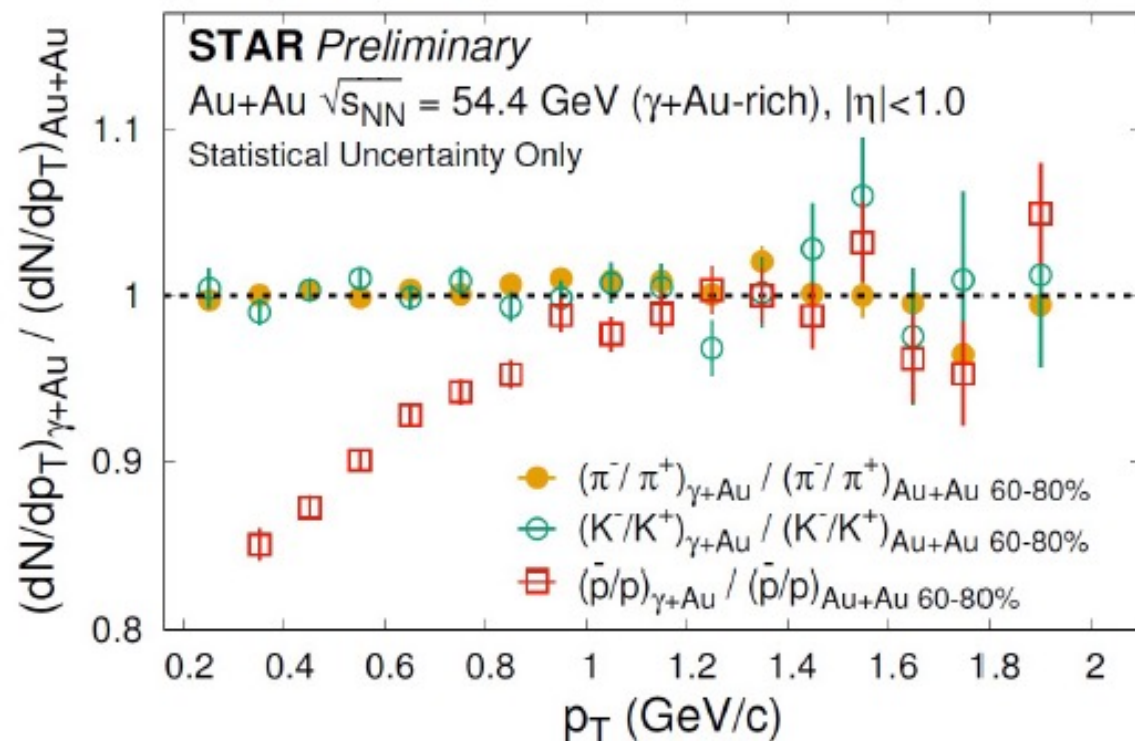
BES data continues with the trend

FIG. 29: The ratio of mid-rapidity inclusive net-protons to half of the number of participants in central heavy-ion collisions as a function of the rapidity shift. The AGS data is taken from Refs. [75, 86], SPS data from Refs. [87, 88, 89], and BRAHMS data from Ref. [90]. The published SPS data have already been corrected for weak-decays, the size of which is of the order 20-25% [88], so we have added 25% to the published net-proton yields to obtain the inclusive ones. Errors shown are total statistical and systematic uncertainties. The dashed line is an exponential fit to the data.





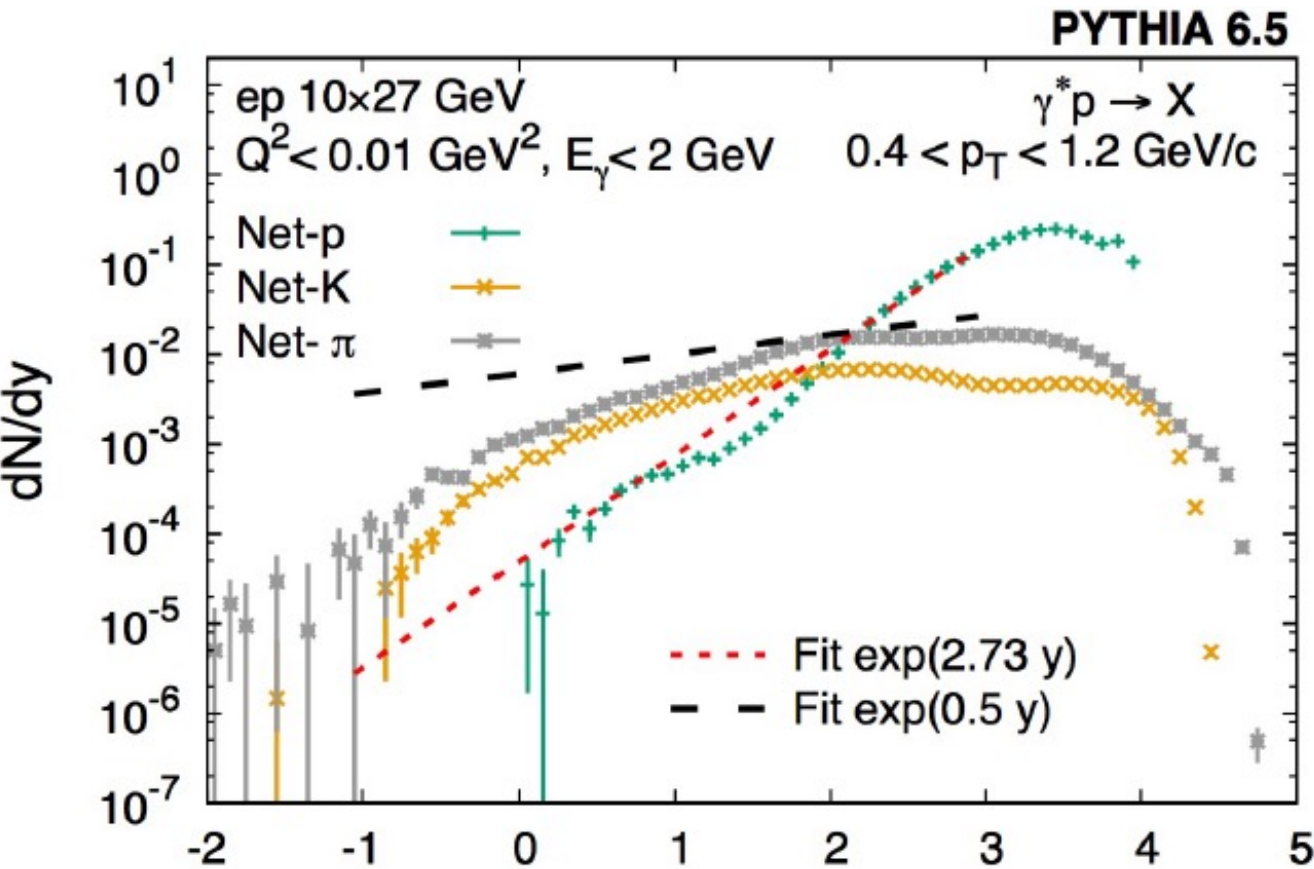
# Comparison with PYTHIA



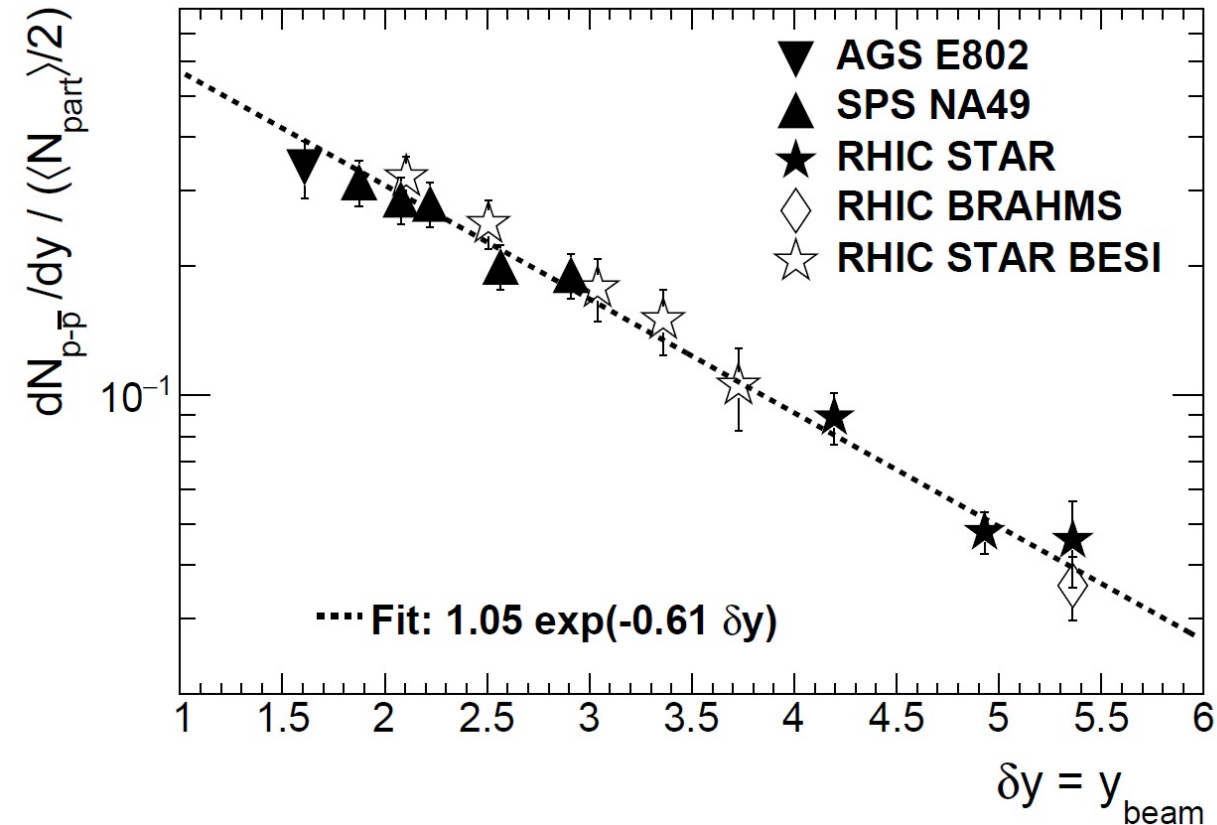
Data: double ratio, PYTHIA is just ratio; model stops no enough baryon and too much charge

PYTHIA6  $\gamma^* p \rightarrow X$  simulation does not include a baryon junction  $\rightarrow$  pion, kaon, and proton ratios are all consistent with 1 within uncertainty

# Measure rapidity dependence of net-protons



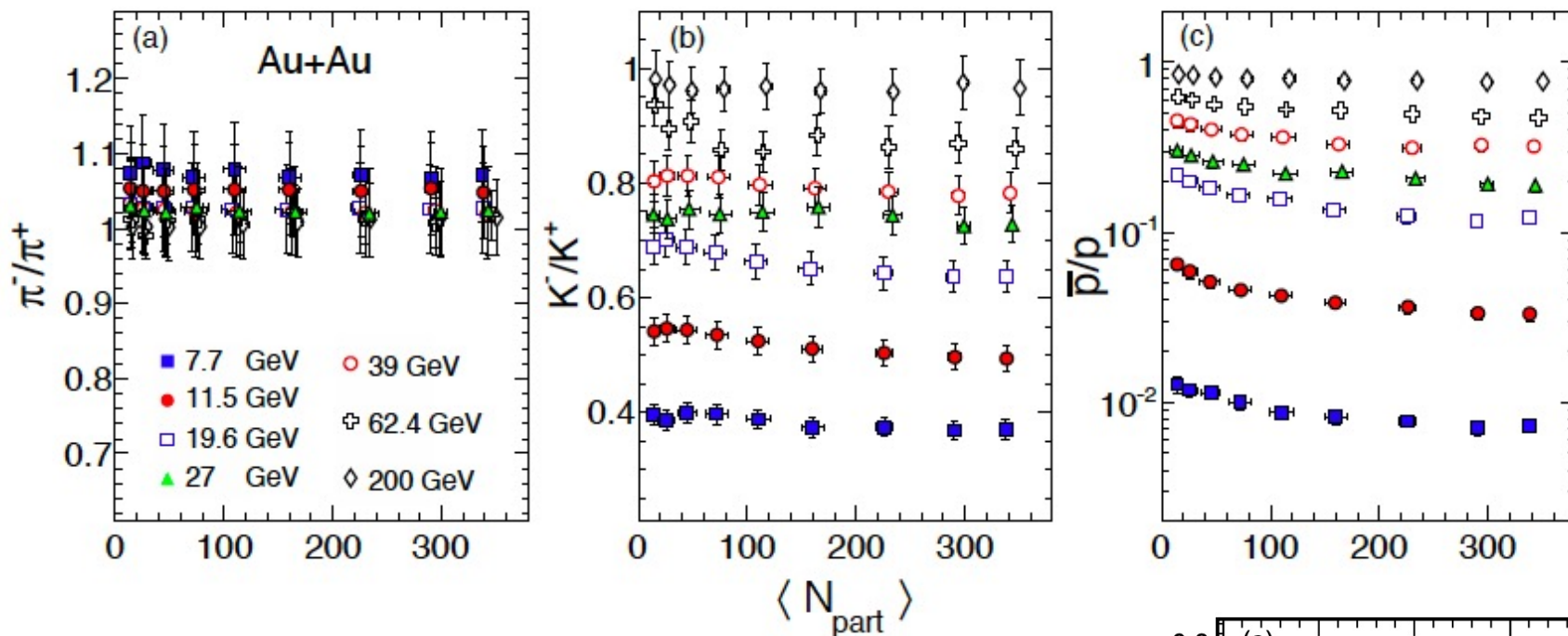
PYTHIA predicts a much bigger asymmetry (P. Tribedy)  
 Baryon junction prediction:  $\exp(-0.5 \cdot y)$  (D. Kharzeev, 1996)



**$dN/dy$  of net-proton rapidity distribution in  $\gamma+A$ :  
 Results by QM2022**

# Negative/positive charged particle ratios

STAR, Phys. Rev. C **96** (2017) 44904

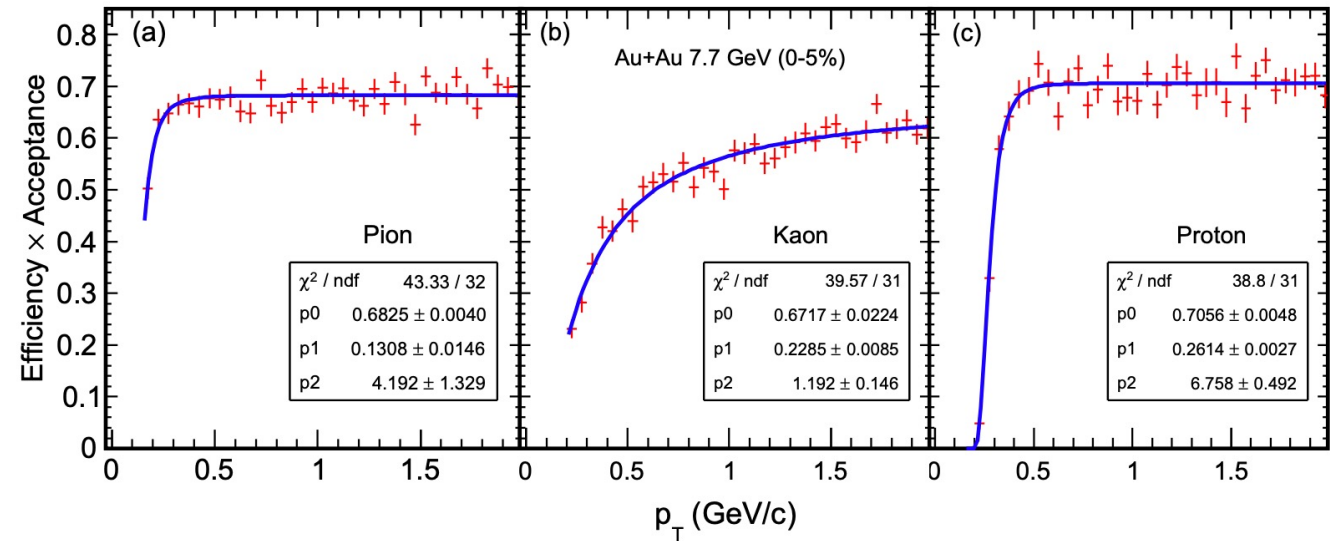


In conventional Au+Au collisions:  
 $\bar{p}/p$  ratio @ **54.4 GeV** is  $\sim 0.4$ ,  
 and decreases with multiplicity  
 $K^-/K^+ \sim 0.8-0.9$

Errors are too large to determine  
 charge net charge at 200 GeV

Isobar data can cancel many of the detector effects  
 net baryon  $B: (p - \bar{p}) \cdot (1 + d/\bar{d}) \cdot (\bar{p}/p)^2$   
 net charge  $Q: \pi^+ + K^+ + p - (\pi^- + K^- + \bar{p})$

$Q = B \cdot (Z/A)$  if baryon number carried by valence quark  
 $Q \ll B \cdot (Z/A)$  if gluon junction carries baryon number  
 Isobar:  $\Delta Q = ? B \cdot (\Delta Z/A)$





# Solenoidal Tracker at RHIC

Artistic rusty representation of past and present



Still an indispensable discovery detector

Crystal Ball prediction of future (literately)

